WRDC-TR-90-2081

DETECTION OF EXCITED STATES BY LASER-INDUCED FLUORESCENCE AND ANALYSIS OF ENERGY TRANSFER

J. BORYSOW and A. V. PHELPS

JOINT INSTITUTE FOR LABORATORY ASTROPHYSICS
QUANTUM PHYSICS DIVISION
NATIONAL INSTITUTE OF STANDARDS AND TECHNOLOGY
BOULDER, CO 80303

September 1990

FINAL REPORT FOR PERIOD OCTOBER 1988 - SEPTEMBER 1989

Approved for public release; distribution is unlimited

AERO PROPULSION AND POWER LABORATORY
WRIGHT RESEARCH AND DEVELOPMENT CENTER
AIR FORCE SYSTEMS COMMAND
WRIGHT-PATTERSON AIR FORCE BASE, OHIO 45433-6563

NOTICE

When Government drawings, specifications, or other data are used for any purpose other than in connection with a definitely Government-related procurement, the United States Government incurs no responsibility or any obligation whatsoever. The fact that the Government may have formulated or in any way supplied the said drawings, specifications, or other data, is not to be regarded by implication, or otherwise in any manner construed, as licensing the holder, or any other person or corporation to manufacture, use, or sell any patented invention that may in any way be related thereto.

This report is releasable to the National Technical Information Service (NTIS). At NTIS, it will be available to the general public, including foreign nations.

This technical report has been reviewed and is approved for publication.

Alan Garscadden

ALAN GARSCADDEN
Advanced Plasma Research Group
Aerospace Power Division
Aero Propulsion and Power Laboratory

Lowell D. Massie

LOWELL D. MASSIE, CHIEF
Power Components Branch
Aerospace Power Division
Aero Propulsion and Power Laboratory

FOR THE COMMANDER

Michael D. Braydich

MICHAEL D. BRAYDICH, Lt Col, USAF
Deputy Director
Aerospace Power Division
Aero Propulsion & Power Laboratory

If your address has changed, if you wish to be removed from our mailing list, or if the addressee is no longer employed by your organization please notify WRDC/POOC-3, Wright-Patterson AFB, OH 45433-6563 to help us maintain a current mailing list.

Copies of this report should not be returned unless return is required by security considerations, contractual obligations, or notice on a specific document.

UNCLASSIFIED

SECURITY CLASSIFICATION OF THIS PAGE

REPORT DOCUMENTATION PAGE

Form Approved OMB No. 0704-0188

1a. REPORT SECURITY CLASSIFICATION Unclassified	1b. RESTRICTIVE MARKINGS
2a. SECURITY CLASSIFICATION AUTHORITY	3. DISTRIBUTION/AVAILABILITY OF REPORT Approved for public release: distribution is unlimited
2b. DECLASSIFICATION/DOWNGRADING SCHEDULE	
4. PERFORMING ORGANIZATION REPORT NUMBER(S)	5. MONITORING ORGANIZATION REPORT NUMBER(S) WRDC-TR-90-2081
6a. NAME OF PERFORMING ORGANIZATION Quantum Physics Division National Inst. of Stds. & Tech. (6b. OFFICE SYMBOL (If applicable))	7a. NAME OF MONITORING ORGANIZATION Wright Research and Development Center Aero Propulsion & Power Lab. (WRDC/POOC-3)
6c. ADDRESS (City, State, and ZIP Code) Boulder, CO 80303	7b. ADDRESS (City, State, and ZIP Code) Wright-Patterson AFB, OH 45433-6563
8a. NAME OF FUNDING/SPONSORING ORGANIZATION (8b. OFFICE SYMBOL (If applicable))	9. PROCUREMENT INSTRUMENT IDENTIFICATION NUMBER MIPR FY-88-N0655
8c. ADDRESS (City, State, and ZIP Code)	10. SOURCE OF FUNDING NUMBERS

PROGRAM ELEMENT NO.	PROJECT NO.	TASK NO.	WORK UNIT ACCESSION NO.
61102F	2301	S1	24

11. TITLE (Include Security Classification)
Detection of excited states by laser-induced fluorescence and analysis of energy transfer

12. PERSONAL AUTHOR(S)
J. Borysow and A. V. Phelps

13a. TYPE OF REPORT	13b. TIME COVERED	14. DATE OF REPORT (Year, Month, Day)	15. PAGE COUNT
Final	FROM 88 Oct TO 89 Sep	1990 September	70

16. SUPPLEMENTARY NOTATION

17. COSATI CODES			18. SUBJECT TERMS (Continue on reverse if necessary and identify by block number)
FIELD	GROUP	SUB-GROUP	nitrogen, ions, diode laser, absorption, discharge, afterglow, internal energy, associative ionization

19. ABSTRACT (Continue on reverse if necessary and identify by block number)

The laser absorption technique was improved through the use of laser diodes and was applied to absorption measurements of the line profiles for the $A\,^2\Pi_u \leftarrow X\,^2\Sigma_g^+$ transition of N_2^+ ions to determine a) the electric field strength in the positive column of pulsed discharges in N_2 from the Doppler shift and broadening, b) the time dependence of the density of ground state N_2^+ ions in pulsed discharges in N_2, and c) the increase in rotational energy of N_2^+ ions drifting through N_2 resulting from the transfer of kinetic energy of the N_2^+ to rotational energy. An analysis of the impact of measurements made under this program on models of nonlinear ionization in N_2 leads to the conclusion that ionization by collisions between pairs of metastable N_2 molecules in the a' state probably make the largest contribution to the growth of instabilities in high-current discharges.

20. DISTRIBUTION/AVAILABILITY OF ABSTRACT	21. ABSTRACT SECURITY CLASSIFICATION
☒ UNCLASSIFIED/UNLIMITED ☐ SAME AS RPT. ☐ DTIC USERS	UNCLASSIFIED

22a. NAME OF RESPONSIBLE INDIVIDUAL	22b. TELEPHONE (Include Area Code)	22c. OFFICE SYMBOL
A. Garscadden	(513) 255-2923	WRDC/POOC

DD Form 1473, JUN 86 Previous editions are obsolete. SECURITY CLASSIFICATION OF THIS PAGE

UNCLASSIFIED

PREFACE AND ACKNOWLEDGMENTS

This work was performed by the Quantum Physics Division, National Institute of Standards and Technology, at the Joint Institute for Laboratory Astrophysics under MIPR FY1455-88-N0655. The work was performed during the period October 1988 through September 1989 under Project 2301 Task S1, Work Unit 24. The Air Force contract manager was Dr. Alan Garscadden, Energy Conversion Branch, Wright Research and Development Center, WPAFB, OH 45433-6563.

We would like to acknowledge the help and advice of K. Gibble in construction of the tunable diode laser and suggestions from A. Gallagher and J. Cooper in the course of the experiment. We would like to thank S. Smith and J. Cooper for the loan of equipment and J. Fenney for help with the computer. The work was supported in part by the Wright Research and Development Center, the National Science Foundation, and by the National Institute of Standards and Technology.

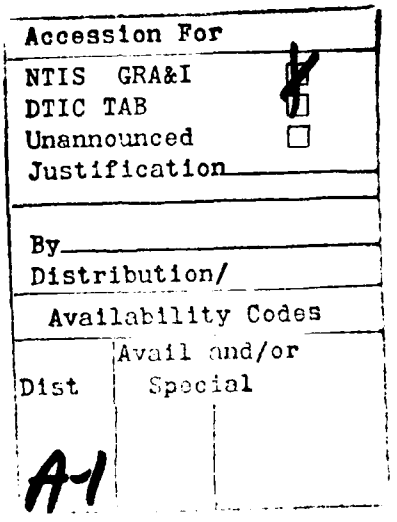

TABLE OF CONTENTS

LIST OF ILLUSTRATIONS

LIST OF ILLUSTRATIONS (Continued)

LIST OF ILLUSTRATIONS (Concluded)

FIGURE PAGE

LIST OF TABLES

SECTION I

I. INTRODUCTION

This report summarizes progress under the project entitled "Detection of Excited States by Laser Induced Fluorescence and Energy Transfer" for the period from 1 October 1988 to 30 September 1989. It is submitted by the Quantum Physics Division of the National Institute of Standards and Technology to the Air Force Wright Research and Development Center. The research was carried out at the Joint Institute for Laboratory Astrophysics with the direct supervision and participation of Dr. A.V. Phelps, Principal Investigator.

The overall objective of this research is to develop diagnostics and models necessary for the measurement and prediction of the properties of electrical discharges in molecular gases which are of interest to the Air Force. For FY 89 we a) continued the development and application of the laser absorption technique to the measurement of time dependent excited state and ion densities in electrical discharges, b) used absorption measurements of the Doppler broadened line profiles for the $A\ ^2\Pi_u \leftarrow X\ ^2\Sigma_g^+$ transition of N_2^+ ions to determine the electric field strength in the positive column of pulsed discharges in N_2, c) completed measurements of the time dependence of the density of ground state N_2^+ ions in pulsed discharges in N_2 using the laser absorption technique, d) developed and applied stabilized diode laser techniques for the measurement of much smaller absorption signals, and e) measured the increase in rotational energy of N_2^+ ions drifting through N_2 resulting from the transfer of kinetic energy of the N_2^+ to rotational energy. Pulsed electrical discharges in molecular gases, such as N_2, are of interest to the Air Force because of their use in devices such as high power switches, electrically excited lasers, and plasma processors. Because of their role in

natural phenomena such as lightning and corona, it is important that one be able to predict the contribution of multistep processes to the growth of ionization in molecular gases such as N_2. Gas discharges play a key role in the production of semiconductors.

An important aspect of this program is the development of nonintrusive diagnostics of electrical discharges in molecular gases. Emphasis on this problem stems from the fact that one of the most fundamental macroscopic parameters of a gas discharge, the electric field, is very difficult to measure without altering the plasma. The traditional approach involves inserting Langmuir probes, but they perturb the plasma. Recent innovations by others include the determination of the electric field from the broadening and shift of emission from high lying excited states of atoms produced by laser excitation of metastables[1]. We show that using a tunable diode laser, the electric field can also be determined with high time resolution from Doppler shifted and broadened absorption by N_2^+ ions.

As our understanding of gas discharges improves it has become important to characterize more completely the energy of ions. We are interested in the internal energy distribution as well as the translational energy of a molecular ion. In particular, we would like to learn how the ion gains its internal energy while drifting in an electric field. This problem is not well understood, especially when charge transfer collisions are the dominant collision processes.

We included in our program:

1) Development of high spectral and time resolution laser absorption methods for measuring properties of molecular ions as described in Section II.

2) Determination of the velocity distribution of molecular ions drifting in the positive column of a discharge and the use of this data to determine the electric field in Sections III and IV.

3) The application of the laser absorption technique for nonintrusive measurement of ion density transient in Section V.

4) Testing of models for the internal energy gained by ions drifting in an electric field in Section VI.

The impact of our previous measurements of N_2 metastable quenching is discussed in Section VII and recommendations for future work are give in Sect. VIII.

SECTION II

EXPERIMENTAL TECHNIQUE

A high density of N_2^+ ions in a uniform electric field in N_2 at a known gas temperature was produced using a pulsed, positive column discharge. A schematic of the discharge tube, laser, and electronics is shown in Figure 1. The discharge tube was in the form of a cross, so as to remove the two cathode regions from the absorption path. The length of the absorption path through the positive column is normally 200 ± 20 mm and can be lengthened by 40 mm by the use of a second anode. We used aluminum electrodes to minimize sputtering.[2] The discharge was operated at a pressure of 0.3 to 1.5 Torr, a current of 0.5 to 1.5 A, and a pulse duration of 5 to 12 μs. The measured E/n, ratio of the electric field to the total gas density, is approximately 100 Td for pure nitrogen and 10 Td for the 10 percent nitrogen - 90 percent helium mixtures used, where 1 Td = 10^{-21} V m^2. The duration of the discharge was chosen to be about equal to the ion lifetime so that the ion density reached roughly its steady-state density. The discharge did not show temporal oscillations or spatial striations. With this choice of energy input the gas heating and excited state production were small. The calculated energy input to the gas during the discharge pulse is from 0.01 to 0.03 eV/molecule. Although most of this energy appears as vibrational excitation,[3] the large vibrational spacing in N_2 of 0.29 eV means that less than 3 percent of the nitrogen molecules will be vibrational excited. Although the recombination of N atoms produced by dissociative excitation depends on unknown wall conditions, measurements in similar discharge tubes[4] suggest sufficiently fast wall recombination of atoms so that dissociation of N_2 is small. The repetition rate of from 10 Hz

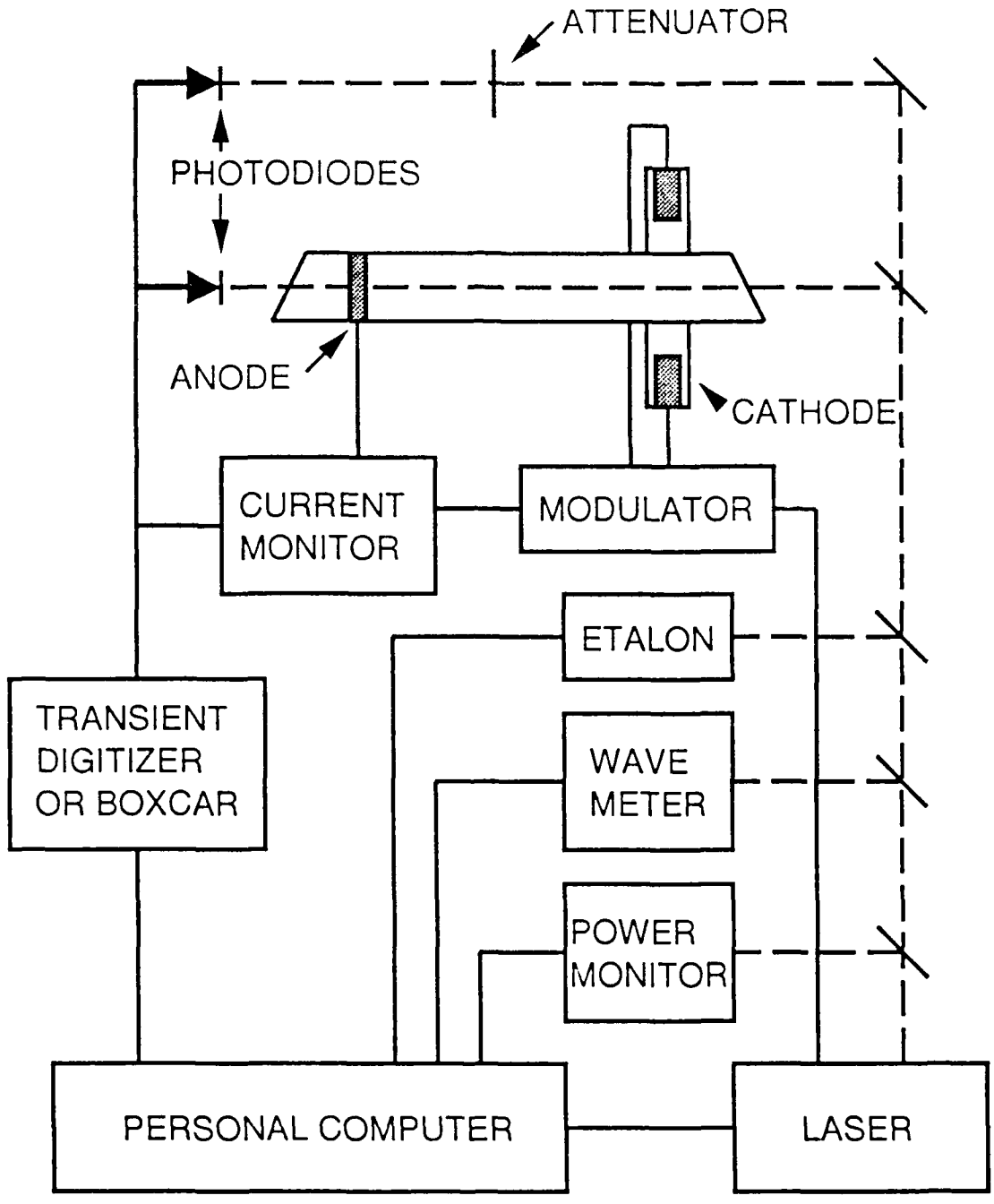

Figure 1. Schematic of the experimental configuration used for Doppler shift and rotational population measurements in N_2.

to 100 Hz ensures that the translational, rotational, and vibrational temperatures will return to close to the wall temperature between pulses.

The average ion density during the discharge calculated for the 14 mm diameter discharge tube and the measured ion drift velocities of Section III is 10^{12} cm^{-3} x I, where I is the current in A and E/n = 100 Td. The estimated uncertainty is ± 10 percent, and arises from the uncertainty in measured current and tube diameter and in published electron and ion drift velocities.

The N_2^+ energy levels and wavelengths of interest in these experiments are shown in Figure 2. In the course of the measurements we used two laser systems. One[5] was based on a commercial, argon-ion-pumped, standing-wave, CW dye laser operating near 689 nm and with a bandwidth of about 1 MHz. This laser was used to study absorption of A $^2\Pi_u \leftarrow$ X $^2\Sigma_g^+$ (v'=3, v"=0) band of N_2^+. The other system was based on the home-made tunable diode laser system with a line width < 1 MHz operating at the wavelength near 780 nm. The laser power on the sample was < 0.5 mW compared to 10 mW maximum available from the diode. The laser was tunable by variation in the effective length of the laser cavity over up to 25 GHz at a fixed value of the electronically regulated diode temperature (± 0.001 K) and current (≈ 10^{-5} percent). We used this laser to measure absorption of the A $^2\Pi_u \leftarrow$ X $^2\Sigma_g^+$ (v'=2, v"=0) band of N_2^+. In both cases, the absolute frequency was measured using a moving-arm interferometer accurate to 300 MHz with respect to a known He-Ne laser[5,6]. A 7.5 GHz confocal etalon and diode served as a relative frequency marker. The laser beam was split in half; one part was sent through the sample and one part was sent through the reference path. The beam passed through the sample cell from 3 to 7 times. In the "single- direction" experiments the beam path formed a loop so that the ion motion relative to the direction of propagation was

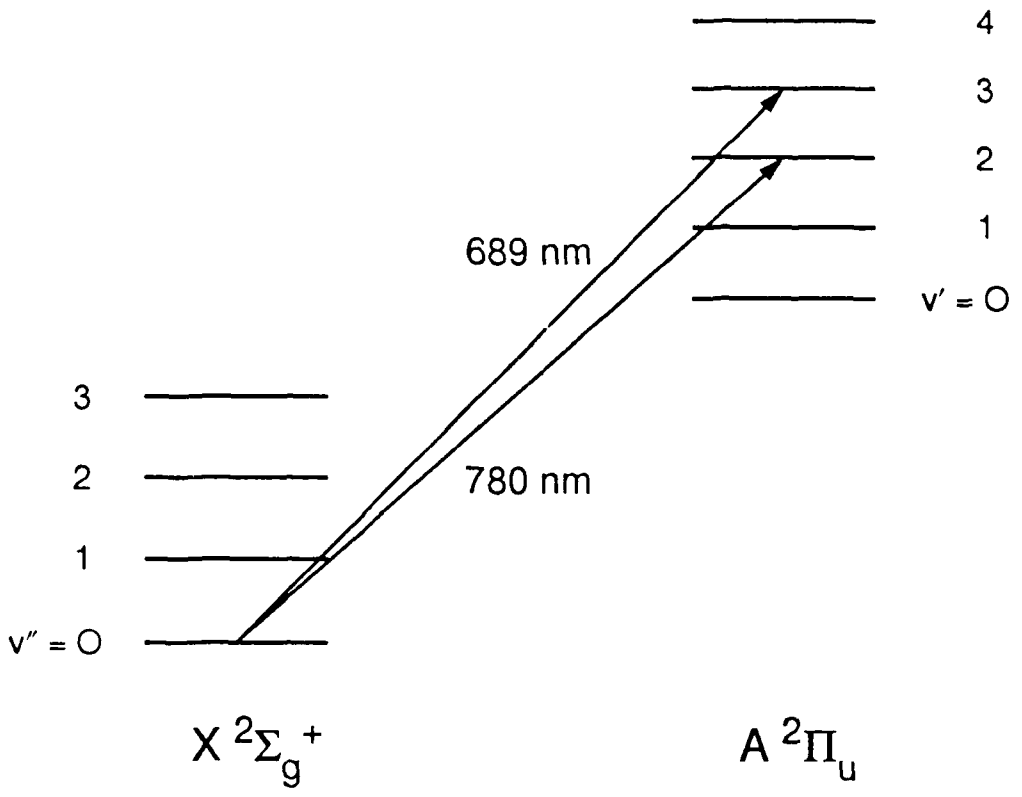

Figure 2. Energy level diagram of the relevant states of N_2^+ showing transitions of interest in this report.

fixed. In the "double-pass" experiments the beam was reflected nearly along the same path so that it alternated direction relative to the ion motion. The beams were directed onto separate photodiodes connected in a differential bridge. A variable attenuator in the reference path was adjusted such that the signals from the diodes were equal when the laser was tuned off resonance. This procedure corrects for any emission from the discharge. The bandwidth of our signal processing electronics was from DC to 160 MHz. Signals from the photodiodes are sent through a preamplifier and amplifier to a boxcar integrator operating in the active-baseline-subtraction mode. For absorption transients measurements the boxcar was replaced by a 100 MHz transient digitizer. The total gain in the system was usually 10^5. With this setup we were able to detect a fractional absorption as small as one part in 10^4 using the CW dye laser, or one part in 10^6 using the laser diode system.

The upper and lower traces of Figure 3 show absorption line profiles obtained with the diode laser a few μs after the pulsed discharge when the electric field is small or zero and during the discharge when the electric field is $\approx$ 100 V/cm. The right-hand line is the $R_1(5)$ ro-vibrational line of the $A^2\Pi_u \leftarrow X^2\Sigma_g^+(v'=2, v''=0)$ transition,[7,8] i.e., the Meinel Band of N_2^+. The center of the unshifted line is indicated by the arrow. The left-hand line is the $Q_1(5)$, $v' = 7 \leftarrow v'' = 6$ line of the $B^3\Pi_u \leftarrow A^3\Sigma_u^+$, 1st positive transition[8] of excited neutral N_2. Comparing the two lines, one sees that in the presence of the electric field the ion line is shifted and asymmetric as the result of the drift of the ions towards the cathode. On the other hand, the position and shape of the neutral N_2 line remained unchanged during the discharge. Figure 4 shows representative absorption profiles for N_2^+ in He. Especially noticeable is the much larger shift of the ion line than in

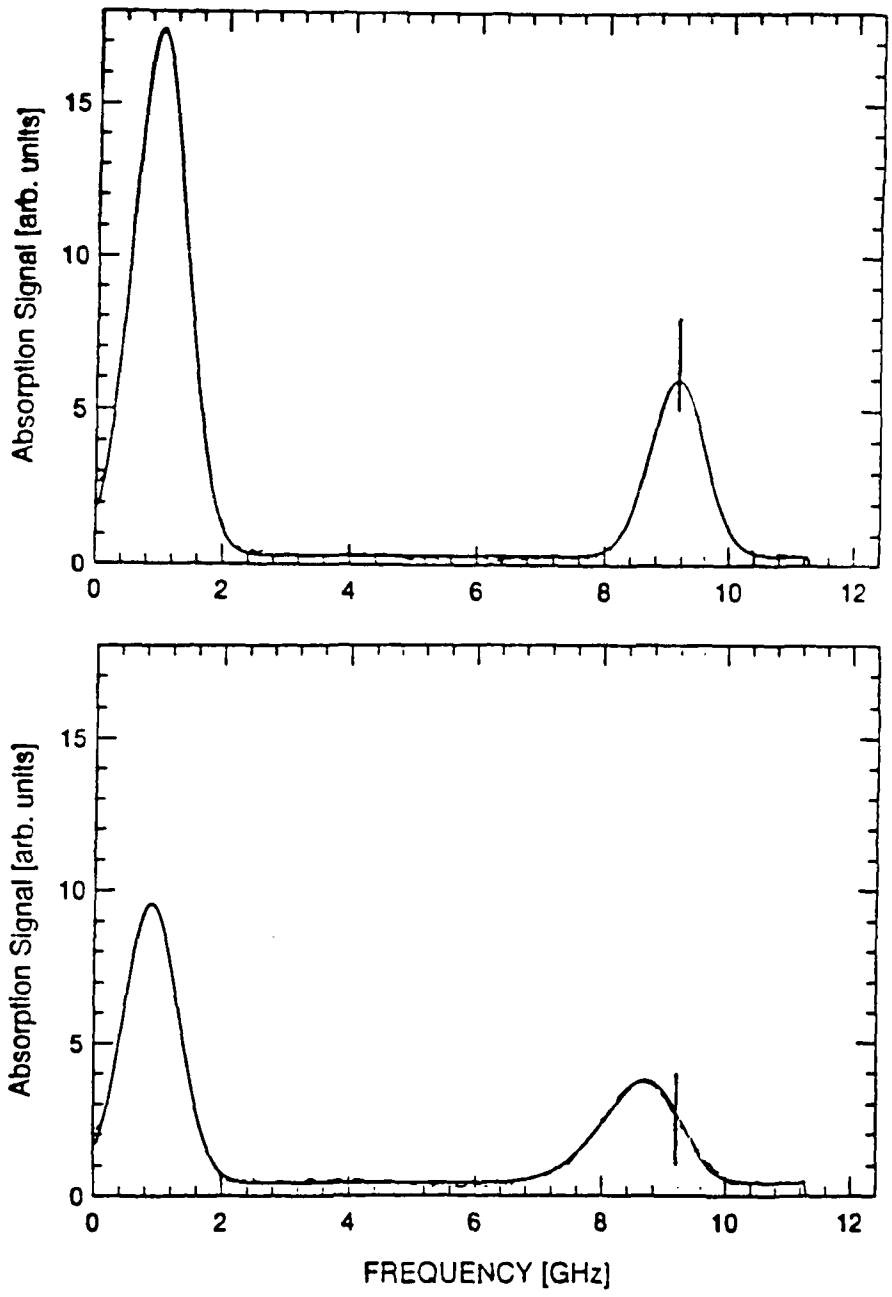

Figure 3. Absorption signals for N_2^+ in N_2. The right-hand line is the $R_1(5)$ line of the $A\ ^2\Pi_u \leftarrow X\ ^2\Sigma_g^+$, $v'=2$, $v''=0$ band of N_2^+ and the left-hand line is the $R_2(9)$, $v' = 7 \leftarrow v'' = 6$ line of the $B^3\Pi_u \leftarrow A^3\Sigma_u^+$, 1^{st} positive transition[8] of excited N_2. The upper trace was obtained during the afterglow, while the lower trace was taken during the discharge.

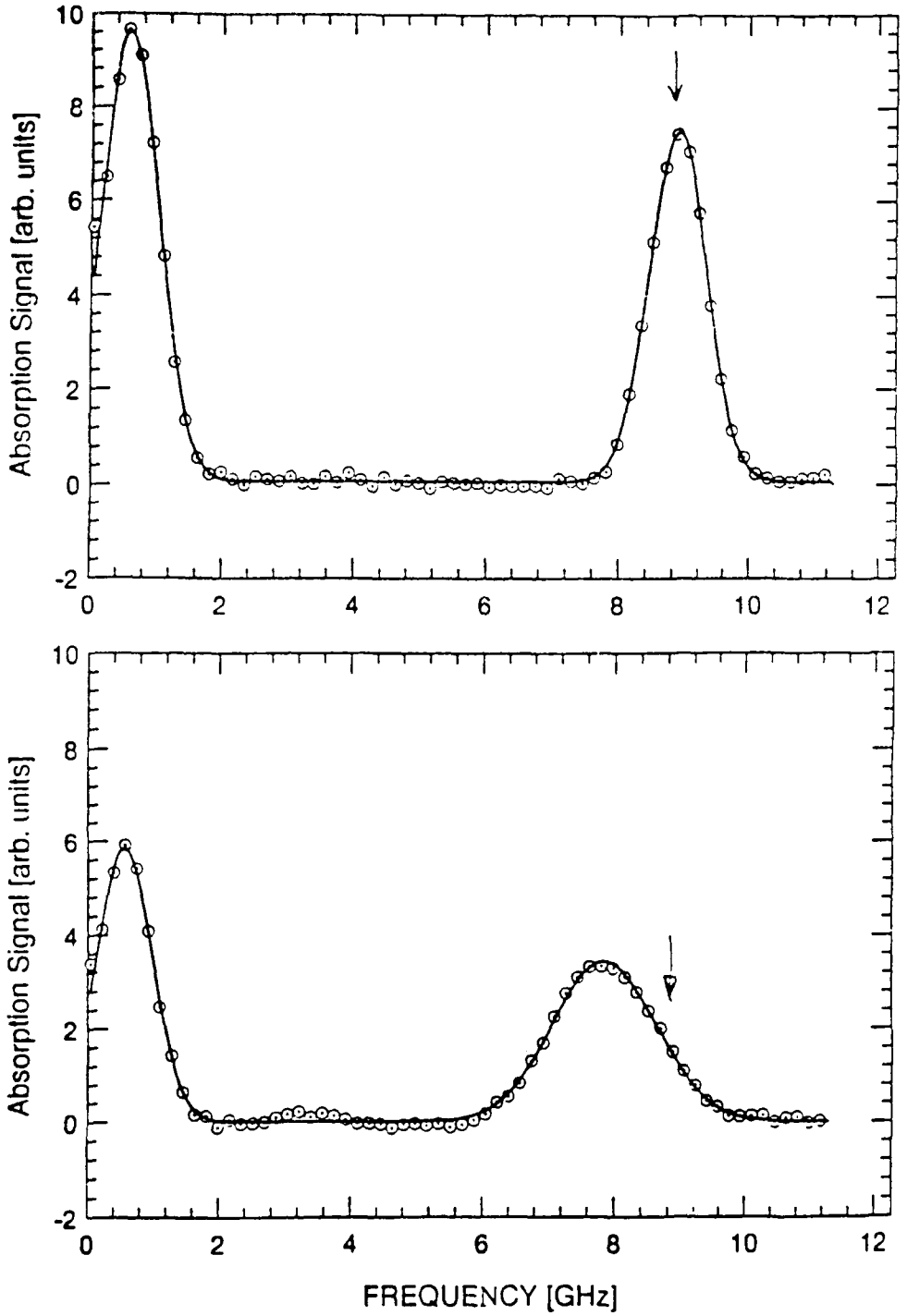

Figure 4. Absorption signals for N_2^+ in He. The lines are as in Figure 3. The upper trace was obtained during the afterglow, while the lower trace was taken during the discharge. The points are experimental data and the solid curves are from a fit of theory.

the case of N_2^+ in N_2.

The gas handling and vacuum system could be pumped to $\approx 2 \times 10^{-4}$ Pa (2×10^{-6} Torr) between runs and $\approx 7 \times 10^{-5}$ Pa (5×10^{-7} Torr) after a mild bake-out. The gas pressures were read with a diaphragm type manometer accurate to $\pm$ 0.01 Torr. Currents and voltages were read from the time independent portions of the digitized waveforms and are expected to be accurate to $\pm$ 10 percent.

In addition to the electric field determinations using Doppler shift methods, the electric field strength in the pulsed N_2 discharges was determined using two floating Langmuir probes[9] spaced 50 mm apart. In order to minimize the perturbation of the plasma, the probes were thin wire (0.2 mm) loops pressed against the glass wall of the discharge tube. The lack of spatial dependence of the visual emission in the vicinity of the probes is consistent with a small perturbation. The time dependent voltages of the loops were measured using high impedance (100 MΩ) oscilloscope probes and the difference voltage determined electronically. Previous experience[10] with these probes and similar discharges in H_2 indicated satisfactory operation.

An important characteristic of the pulsed discharges used in these experiments is their uniformity in the axial direction. To test this uniformity, measurements were made of the transient emission at 391.4 nm from N_2^+ at about 1 cm from the anode and 20 cm from the anode toward the cathode. Emission was measured with a photomultiplier using an interference filter centered at 391.4 nm with a 10 nm bandwidth. Care was taken to insure that changes in the collection geometry were small. Figure 5 shows emission transients taken at nitrogen pressure of 0.5 Torr and current of 1.5 A. The traces are very similar. Since the excitation coefficient for this state[11]

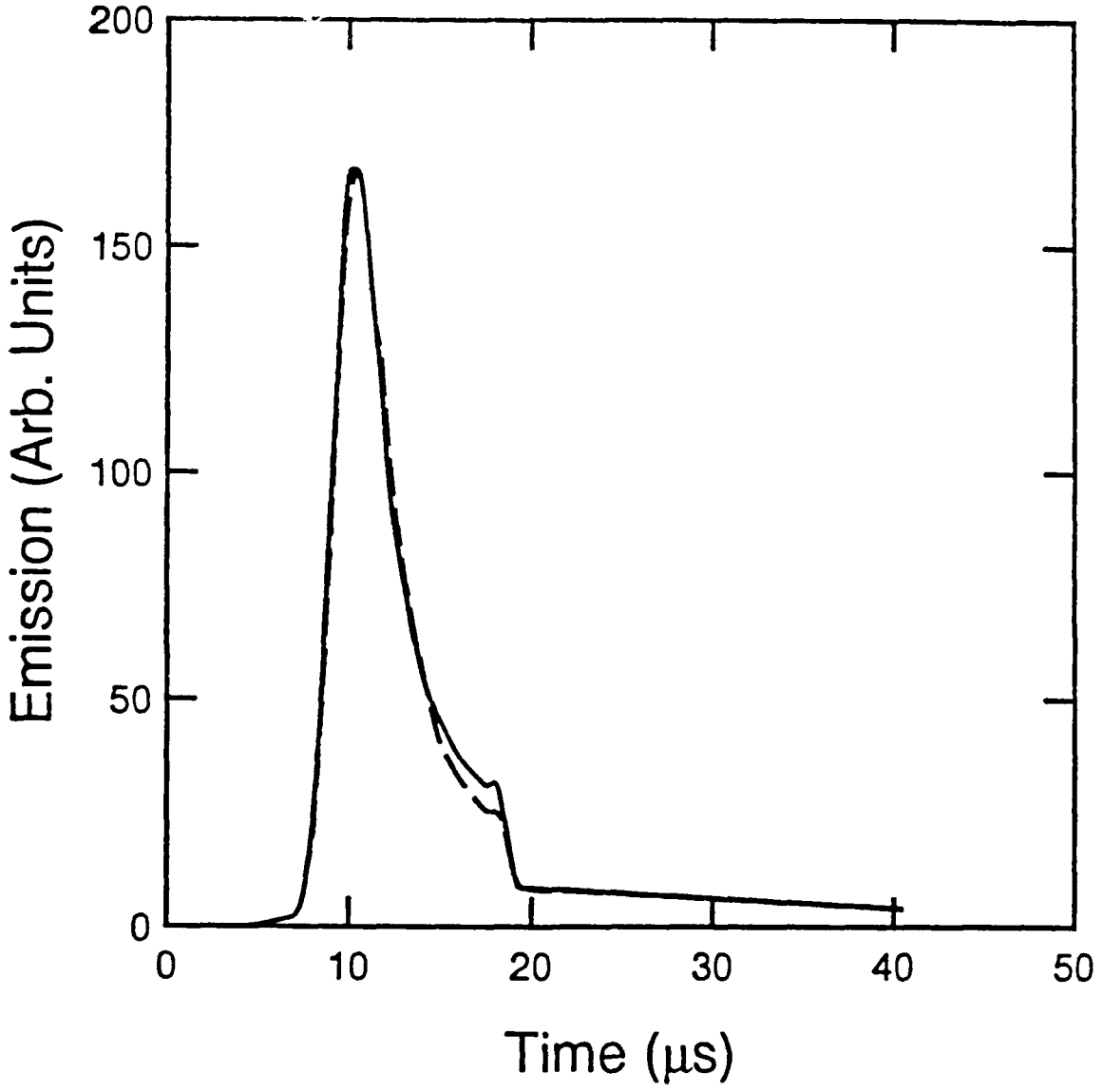

Figure 5. Emission at 391.4 nm from N_2^+ A $^2\Pi_u$ ions at a position near the anode and near the cathode end of the positive column showing the uniformity of excitation along the discharge. p = 1 Torr, I = 1.7 A.

varies rapidly with E/n for discharge conditions, we concluded that the electric field is constant to ≈ 10 percent along the discharge tube.

The results of the analyses of the ion motion under the influence of the electric field obtained from the Doppler broadened and shifted absorption transition of the Meinel Band of N_2^+ are presented in Sections III and IV. The populations of different rotational states were obtained from the integrated absorption profiles of the ro-vibrational transitions $A\ ^2\Pi_u \leftarrow X\ ^2\Sigma_g^+$ ($v'=2$, $v''=0$) of N_2^+ in the vicinity of 780 nm and the results are presented in Section VI.

SECTION III

ELECTRIC FIELD IN THE POSITIVE COLUMN

Traditionally, Langmuir probes have been used to measure the electric field in a plasma.[9] This approach perturbs the plasma.[12] In recent years, there have been several nonintrusive measurements of an electric field. Wieman and Hansch[13] observed the Stark splitting in deuterium and in H_2 discharges. Ganguly et al.[1] applied the Stark splitting technique to very high levels of He excited by a laser from the metastable state. The use of Stark splitting by observation of resolved spectra was applied for electric fields as low as 100 V/cm and by observation of line merging was applied to fields of $\approx$ 5 V/cm. Doughty and Lawler[14] used the optogalvanic effect to measure Stark splitting for electric fields to $\pm$ 10 V/cm at 400 -1000 V/cm. Mocre et al.[15] measured the electric field by observing the Stark mixing in the electronic transition of BCl. A similar approach was developed by Derouard and Sadeghi utilizing the NaK molecule.[16] For discharges containing these molecules, this approach has been used for electric fields as low as 20 V/cm. Haese, Pan, and Oka[17] used infrared laser absorption for measurements of the Doppler shift to determine the mobility of ArH^+ in the positive column of a dc discharge. Radunsky and Saykally[18] measured an axial electric field by observation of the Doppler shift of drifting ions in the poorly known electric field of a low frequency discharge. We will show that by measuring the Doppler shift of N_2^+ absorption spectra in a dc positive column discharge one can determine electric fields to at least as low as 3 V/cm.

We have applied two methods of analyzing absorption profiles to obtain the axial electric field:

1. Spectral moment method. This method is based on the calculation of mean frequency shift $\Delta\nu$ of the absorption line as the ratio of the first moment to the zeroth moment using the relation

$$\Delta\nu = \frac{\int d\nu\ I(\nu - \nu_0)\ (\nu - \nu_0)}{\int d\nu\ I(\nu - \nu_0)} \quad , \qquad (1)$$

where ν_0 is the frequency of the line center as determined in the absence of an electric field and $I(\nu - \nu_0)$ is the measured absorption line profile. The frequency of the center of the unperturbed line ν_0 is assumed to be the center of the absorption profile measured after the discharge voltage is reduced to zero, i.e., ν_0 is adjusted to make $\Delta\nu = 0$ in Equation (1) for $I(\nu - \nu_0)$ taken well after the end of the applied voltage pulse.

2. Convolution method. The convolution method assumes that the ion velocity distribution can be represented by the convolution of thermal and high field velocity distributions. This problem is discussed in more detail in Section IV. A minimum of three parameters is required to describe the resultant velocity distribution. The parameters of the velocity distribution plus those describing the background signal and absolute amplitude of the absorption signal are adjusted to give the best fit of the model to the measured line absorption profile.

The moment method has a major advantage over other techniques in that it does not require any assumptions as far as velocity distribution of ions is concerned and is very simple to apply. It does not involve a complicated fitting procedure. It provides the mean Doppler shift, which equals the drift velocity of an ion. On the other hand, the line fitting technique can be applied for overlapping spectral lines. This feature is particularly

interesting for systems like N_2^+ in N_2 where in every spectral region there are large numbers of absorption lines from excited neutral molecules.

We use previously measured drift velocities[19] as shown in Figure 6 to convert our measured drift velocities to E/n values and then to the magnitude of the electric field. The resulting E/n values versus nR values are shown by the crosses in Figure 7 for pressures from 0.25 Torr to 2.0 Torr. The E/n results are plotted versus nR, rather than pressure to allow scaling of theory to these experiments. Here n is the gas density and R is the radius of the discharge tube. The measured field is calculated from the ion drift velocity at the end of the pulse. This value was assumed to be equal to the steady-state value.

In Figure. 7 the open points show E/n values determined from the fitting method. The results closely follow numbers obtained from the moments method.

Electric field measurements by means of the probes are shown in Figure 7 as circles. An example of the transient potential difference between two probes is shown in Figure 8. The "steady-state" electric field is calculated from the potential difference at the end of such waveforms and the distance between the probes. The results are systematically below the steady-state electric field calculated theoretically[20] and slightly below the measurements based on the observation of the absorption profiles.

The measured E/n values obtained from analysis of the Doppler shifted absorption lineshapes fall systematically below calculated E/n values at the higher nR. One possible explanation is that after the applied discharge voltage is turned off there is still some residual electric field which causes the ions to drift toward the cathode and produce an error in the value of ν_0 in Equation (1). This error becomes more serious as the frequency shift

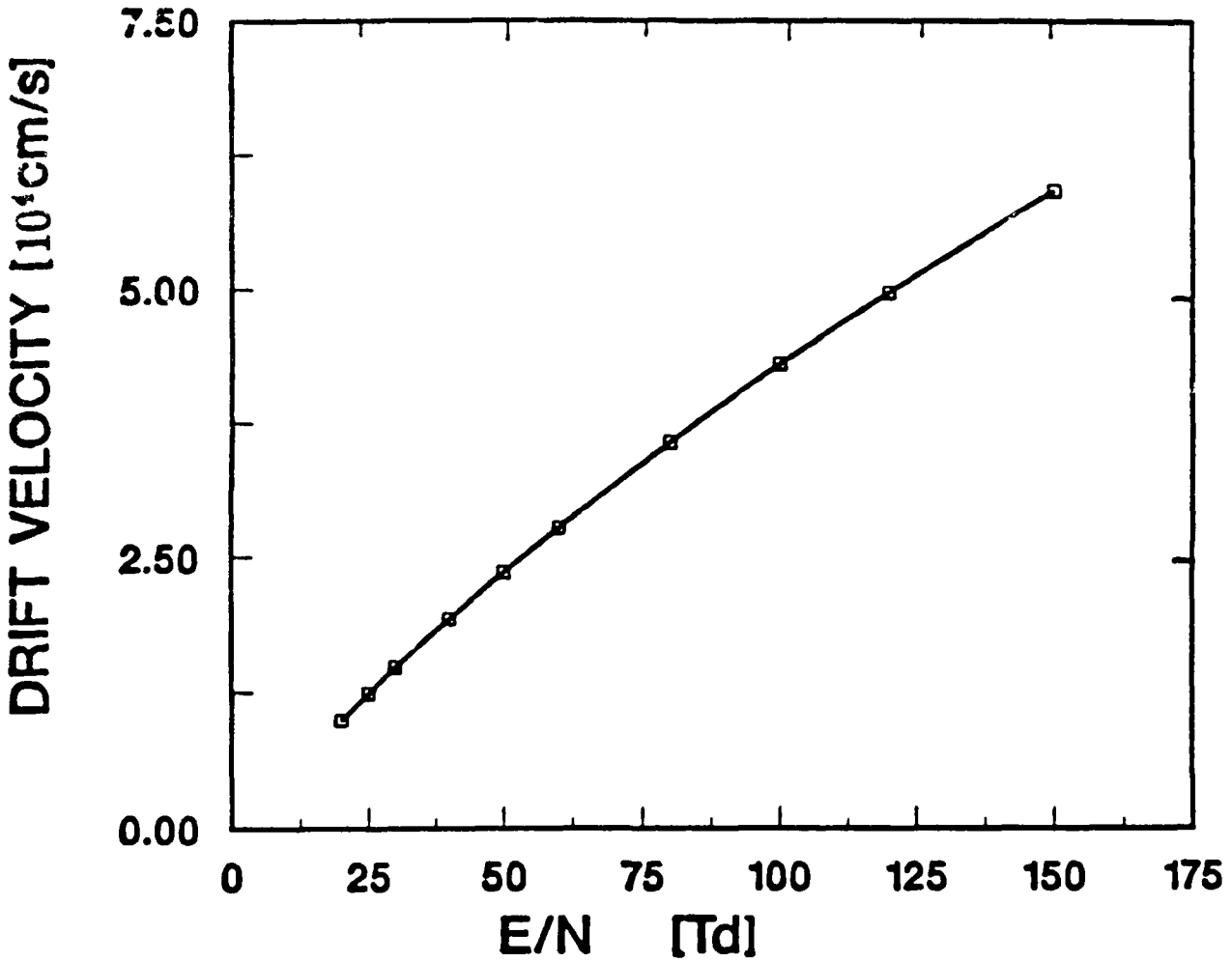

Figure 6. Drift velocity for N_2^+ in N_2 from Ellis et al.

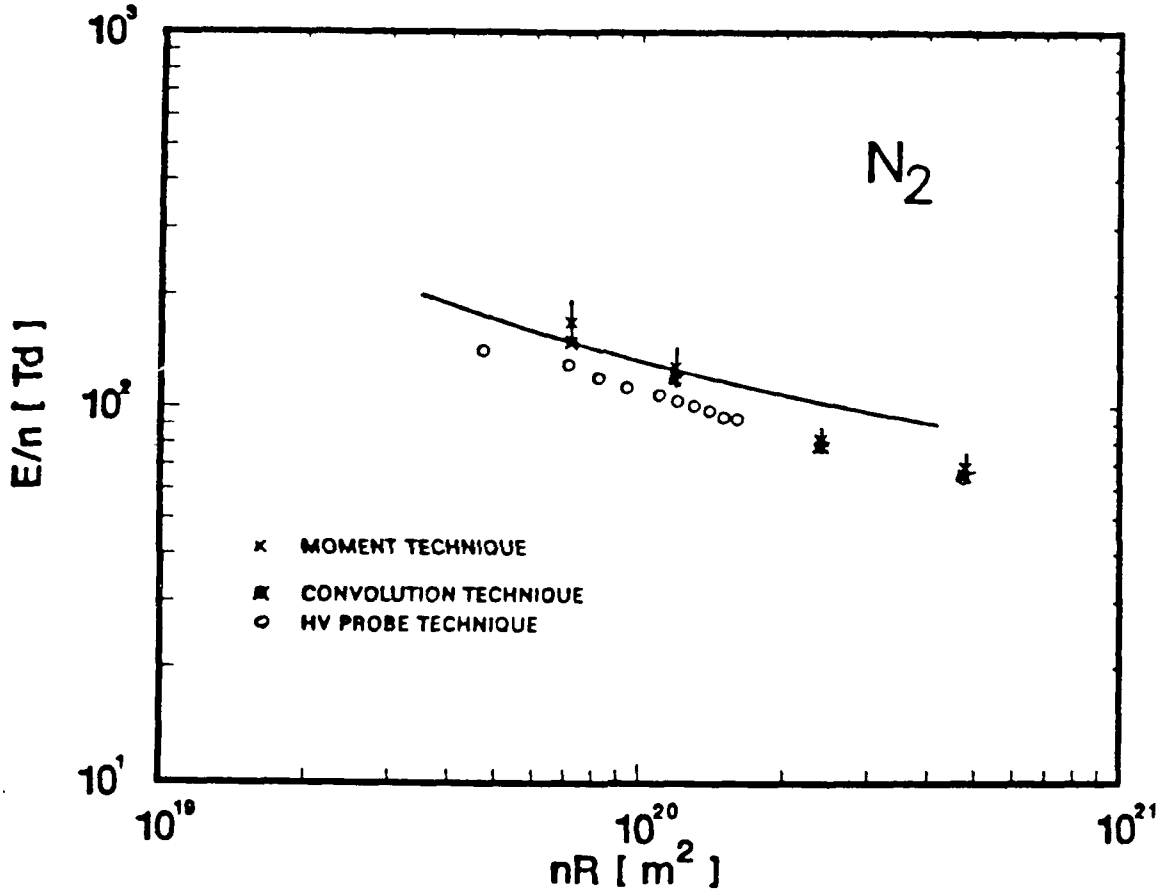

Figure 7. Measured and calculated E/n versus nR for pure N_2 positive column. The points are our experimental results, while the smooth curve is calculated using the procedures of Ref. 6.

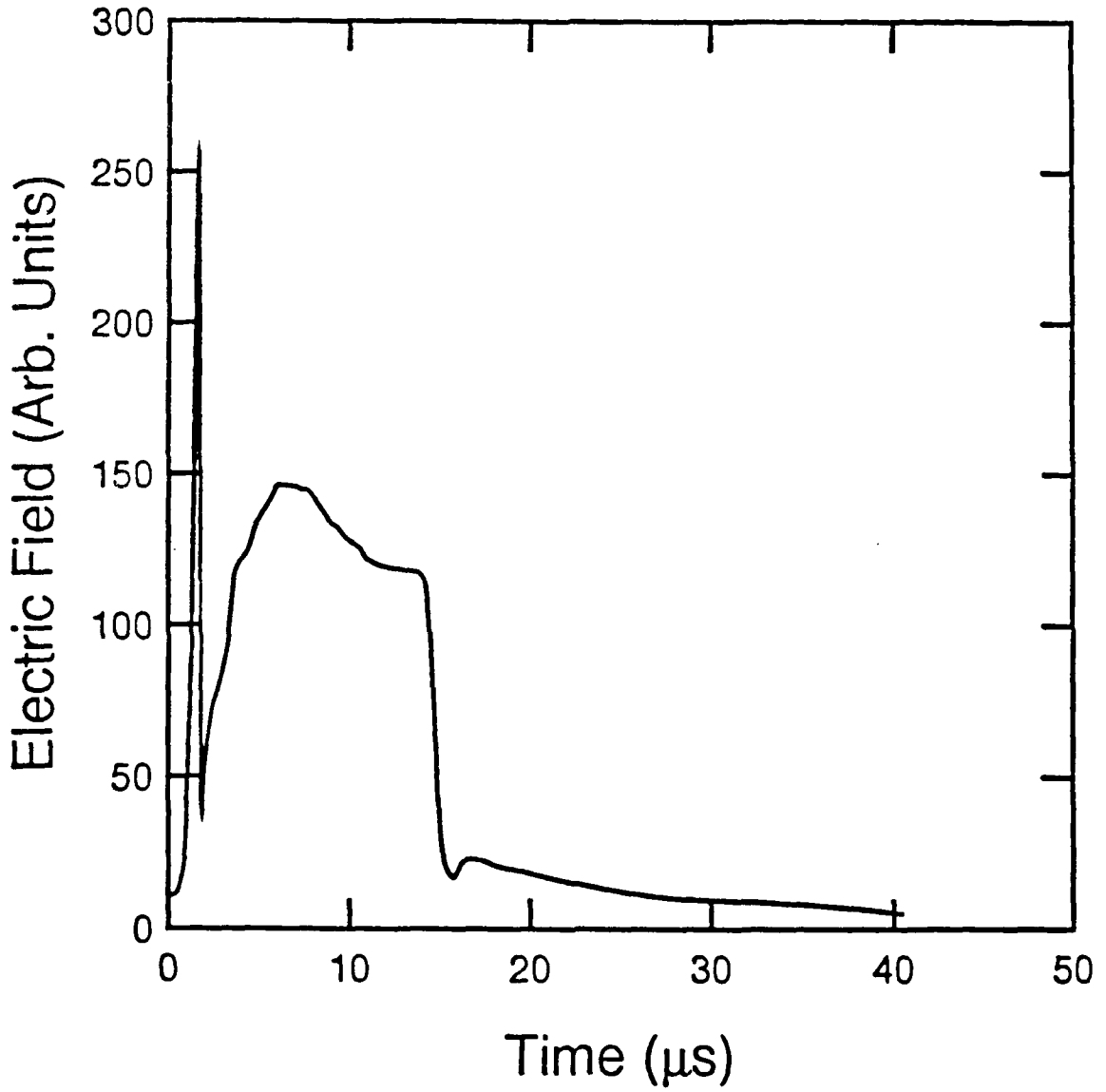

Figure 8. Transient voltage difference between wall probes for p = 1 Torr and I = 1.6 A.

decreases at the lower E/n. As we will show in Section IV, there is some evidence to support this hypothesis.

Our methods make possible determinations of the electric field at different times during the pulsed discharge. An example of such time-resolved E/n determinations is shown in Figure 9. The experimental data were taken using the tunable CW dye laser operating near 689 nm. The time dependence of an electric field during the pulsed discharge is in reasonably good agreement with laser measurements. Since we obtain a significantly better signal to noise level with the diode laser than with the dye laser, we expect to be able to obtain either more accurate determinations of the electric field or reasonably accurate electric field values with a much higher time resolution than that shown in Figure 9.

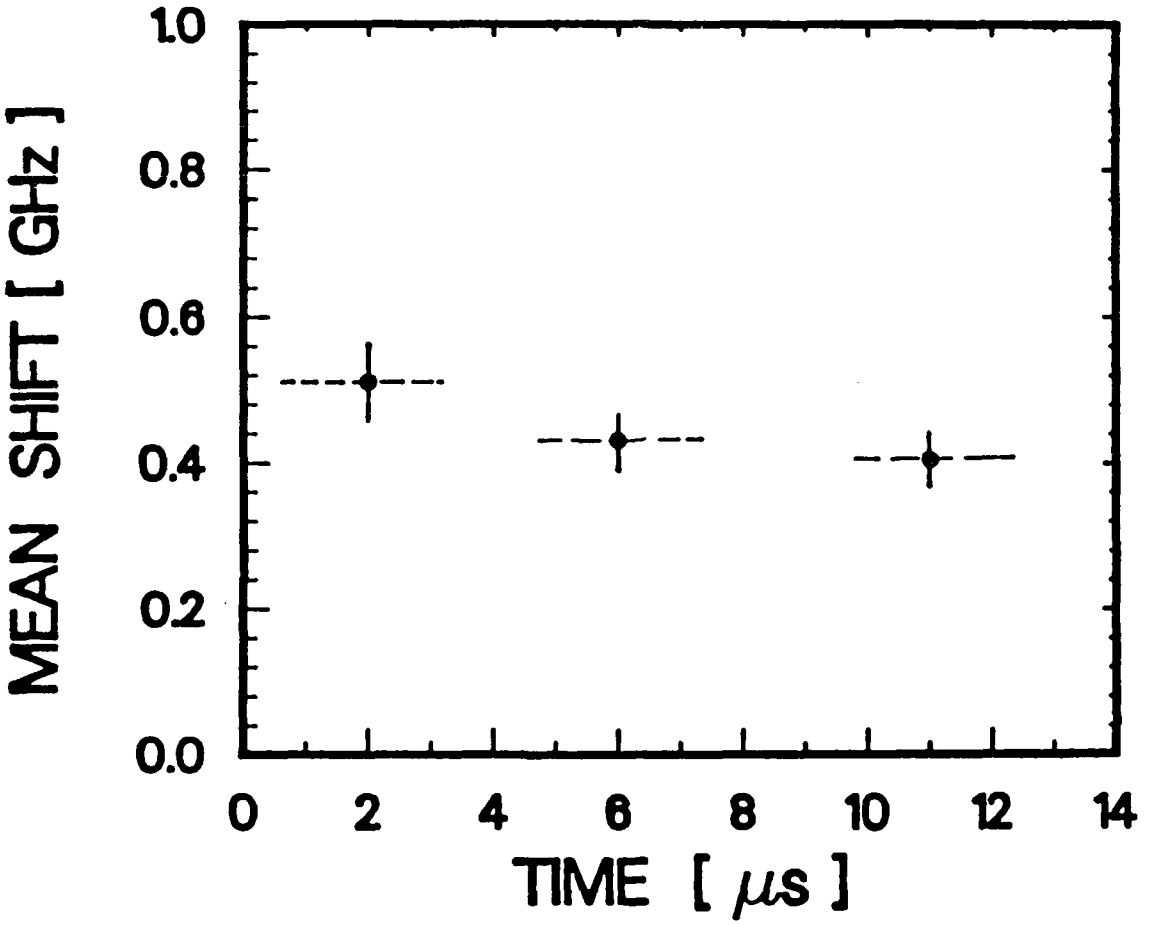

Figure 9. Time dependence of mean Doppler shift during pulsed discharge. p = 1 Torr and I = 1 A.

SECTION IV

VELOCITY DISTRIBUTION OF IONS

Little is known about the velocity distribution of ions in their parent gas at moderate electric fields where the gain in velocity between collisions is comparable with thermal velocity of ions. Since solutions of the Boltzmann equation for ions in the presence of the charge transfer collisions do not appear to exist, we postulate that the velocity distribution of such ions is the convolution of thermal and high field velocity distributions. For the high field limit we adopted the solution for the case in which charge transfer is the dominant ion-neutral collision process and the cross section is independent of ion energy.[21,22]

The high field or cold gas approximation is expressed by the assumption that the thermal distribution of velocities is a δ function. The solution[21,22] of the Boltzmann equation for the ion velocity distribution $h(\vec{v})$ then takes the form

$$h(\vec{v}) = C\,\delta(v_x)\,\delta(v_y)\,s(v_z)\exp\left(-\frac{n\,\sigma\,v_z^2}{2\,a}\right), \qquad (2)$$

where v_x, v_y, and v_z are the x, y, and z components of velocity, $s(v_z)$ is the step function, σ is the charge transfer cross section, $a \equiv eE$, and the electric field E is in the z direction. This expression for the velocity distribution of ions moving in the high electric field is a one-dimensional, one-sided Gaussian with the maximum at zero velocity.

The convolution of the high field solution of the Boltzmann equation (half Gaussian) with the thermal distribution (isotropic, full Gaussian) is

shown in Figure 10. Here the v_z values have been converted into frequency shifts using the Doppler relation that

$$\nu - \nu_0 = v_z/\lambda_0, \qquad (3)$$

where ν_0 and λ_0 are the frequency and wavelength at the center of the unperturbed molecular line. The example shown is for the case in which the width of the half Gaussian was approximately twice of the width of the thermal distribution. The resultant lineshape is a shifted, slightly asymmetric profile. The experimental absorption profile resulting from such a velocity distribution is shown in the lower trace of Figure 3. The circles are samples of experimental data and the solid lines are fitted profiles. In fitting the profile to the measured ion line profile obtained during the discharge, only the parameter describing the width of the half Gaussian contribution to the velocity distribution from the electric field was varied. The width of the thermal Gaussian was taken from a fit to the neutral absorption line profile. The line shape of the N_2^+ transition in the upper trace of Figure 3 taken 2 μs after the end of the discharge pulse can be fitted very accurately by a Gaussian profile. The profile is slightly wider, by about 12 K, than profile of the first positive $B\ ^3\Pi_g \leftarrow A\ ^3\Sigma_u$ transition of neutral nitrogen, which corresponds to 293 K. We propose that this difference means that after the discharge there is still some electric field present.

In order to test for nonthermal ion velocity distributions in the afterglow, we show in Figure 11 absorption profiles measured 1μs, 15μs and 120μs after the discharge has been switched off. The width of the ion line becomes narrower with time and at 120 μs approaches the width of the neutral

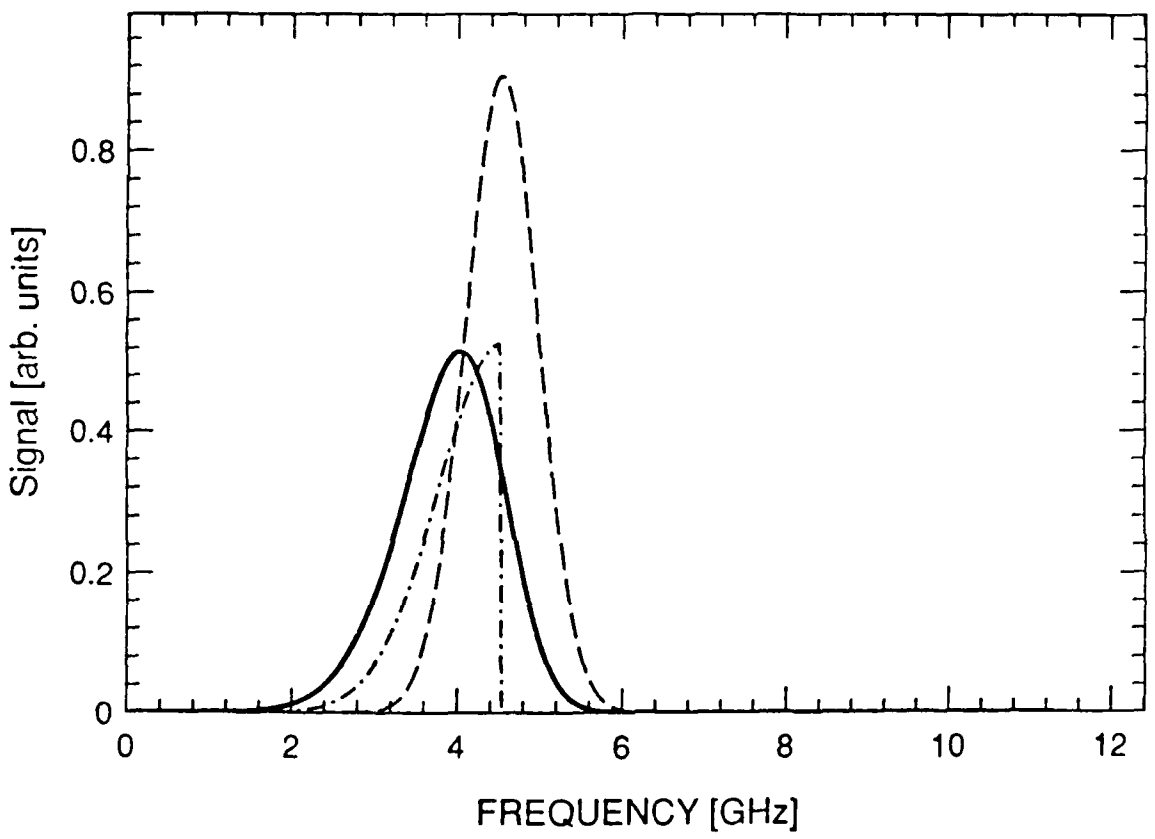

Figure 10. Illustration of folding procedure used to obtain the Doppler profile (solid) from the thermal distribution (dashed) and the one-sided drift distribution (dot-dash).

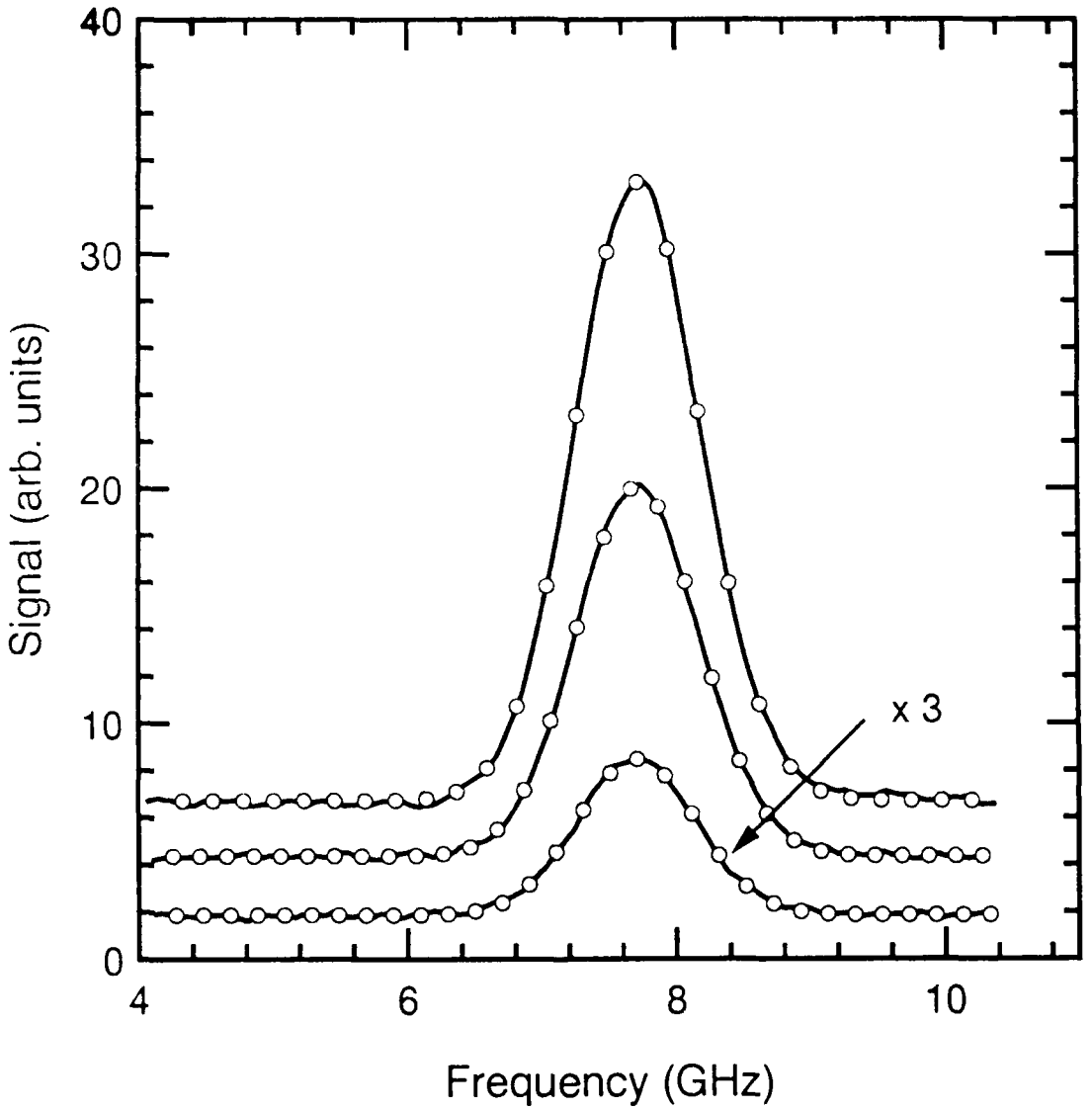

Figure 11. Experimental and fitted absorption profiles taken at various times after turning off current pulse. The solid curve is the experimental data and the points are the results of fitting Gaussians to the various data sets. The time delays are 1 μs, 15 μs, and 150 μs for the data sets starting from the top.

line. The measurements at times later than 120 μs were not reliable because of the small absorption signal resulting from the low ion densities.

We have recorded line shapes and determined the drift velocity of N_2^+ in the positive column discharge for the rotational levels up to a quantum number 20 at pressures from 0.3 Torr to 1.5 Torr. We concluded that to within the experimental accuracy of $\pm$ 7 percent, the drift velocity of the N_2^+ in N_2 does not depend on the rotational quantum number of the molecular ion. A similar lack of dependence of the drift velocity on the rotational quantum number was found for N_2^+ in He. These results differ from those for CO^+, where Saykally and coworkers[18,23] reported that the drift velocity of CO^+ in He is strongly dependent on the rotational state of the ion.

We have also made measurements of Doppler profiles for N_2^+ in He as shown in Figure 4. Although the primary purpose of the measurements in He was to compare our results for the internal energy of the N_2^+ with previous results in Section VI, we show in Figure 4 a fit of a Gaussian to the measured line profile. Although there appears to be no detailed theory for the velocity distribution of N_2^+ in He, the displaced Gaussian given by the fit to the data of Figure 4 is typical of theory[24] and experiment[25] for atomic ions in He. Using published drift velocity measurements for N_2^+ in He, one can determine the E/n values for the conditions of our experiments for use in the analyses of Section VI.

SECTION V

TRANSIENT MEASUREMENTS OF ION DENSITY

In this section we are concerned with transient measurements of absorption at fixed laser frequency, rather than the frequency dependence at fixed times as in Sections III and IV. By observing the transient absorption at various frequencies we learn about the time scale of velocity redistribution. We have also measured time dependence of the ion density and related it to models of the ion loss processes.

A. Transient behavior of the ion velocity distribution.

Since the band width of the laser and the natural line width are both significantly less than the Doppler width of the absorption line, measurements of absorption at fixed laser frequency are sensitive to a small group of N_2^+ ions which have components of their velocity in the direction of propagation of the laser which match the Doppler shifted laser frequency. Consider first an experiment in which the laser is tuned to the middle of an unshifted N_2^+ transition so as to detect absorption by slow ions. There is little absorption when the electric field is on because the high ion temperature depletes the slow ion population. After the discharge is turned off there is a sudden increase of absorption by ions in the slow velocity group. This is due to the fact that when the electric field is reduced the ions are slowed down very quickly in collisions with cold N_2. In these experiments the N_2 gas remains at near room temperature during the short discharge pulse.

The measurement reported in this subsection were made using absorption for ro-vibrational transitions for $A\ ^2\Pi_u \leftarrow X\ ^2\Sigma_g^+$ ($v'=3$, $v''=0$) of N_2^+ in the

vicinity of 689 nm. The experimental apparatus was the CW dye laser with a bandwidth less than 1 MHz pumped by an Ar^+ laser.

At the top of Figure 12 one sees the cooling of the N_2^+ as a sharp increase in absorption at the end of the discharge. The heating of the ions occurs while the ion density is still very small. In order to emphasize the transient periods, Figure 13 shows the derivatives of the absorption transient and the current transient for pressures of 0.3 Torr. The derivative of the absorption at the end of the pulse closely follows the derivative of the current. If the duration of the decay of absorption corresponded to the time required for velocity redistribution, the duration of the derivative of absorption would decrease with increasing pressure because of the increase in the rate of ion-neutral collisions. From the observed lack of such a pressure dependence, we conclude that the velocity redistribution of molecular ions in collisions with N_2 is faster than the time of switching off the discharge.

The lowest trace in Figure 12 shows the transient absorption when the laser is tuned to one side of the line so as to observe absorption by fast moving ions. There are an appreciable number of ions in this velocity group when the electric field is on, but when the discharge is turned off the ions suddenly slow down in collisions with cold N_2. Instead of a sharp peak, cooling results in a sharp dip in absorption as ions leave this high velocity group. Figure 12 also shows absorption transients for a velocity group for which the population remains constant after the switching off of the electric field. This time the laser was tuned to the side of the Doppler absorption profile of N_2^+. After the sharp increase or decrease of the population of ions in the observed velocity group, there is a slow decay of population in time.

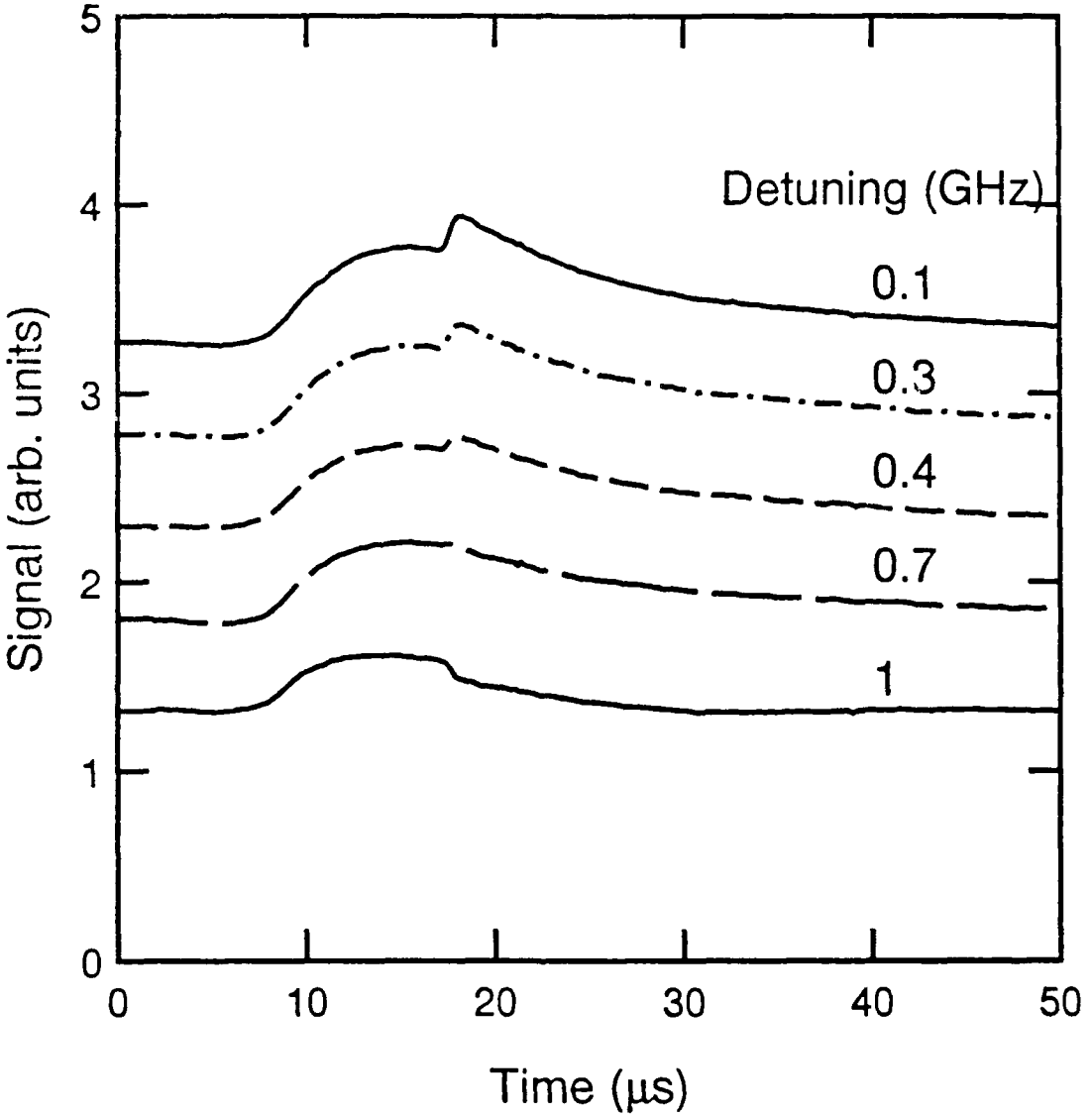

Figure 12. Transient absorption by N_2^+ for various laser detunings. The upper trace is for the laser tuned near line center. The detuning toward the wings increases with decreasing trace position.

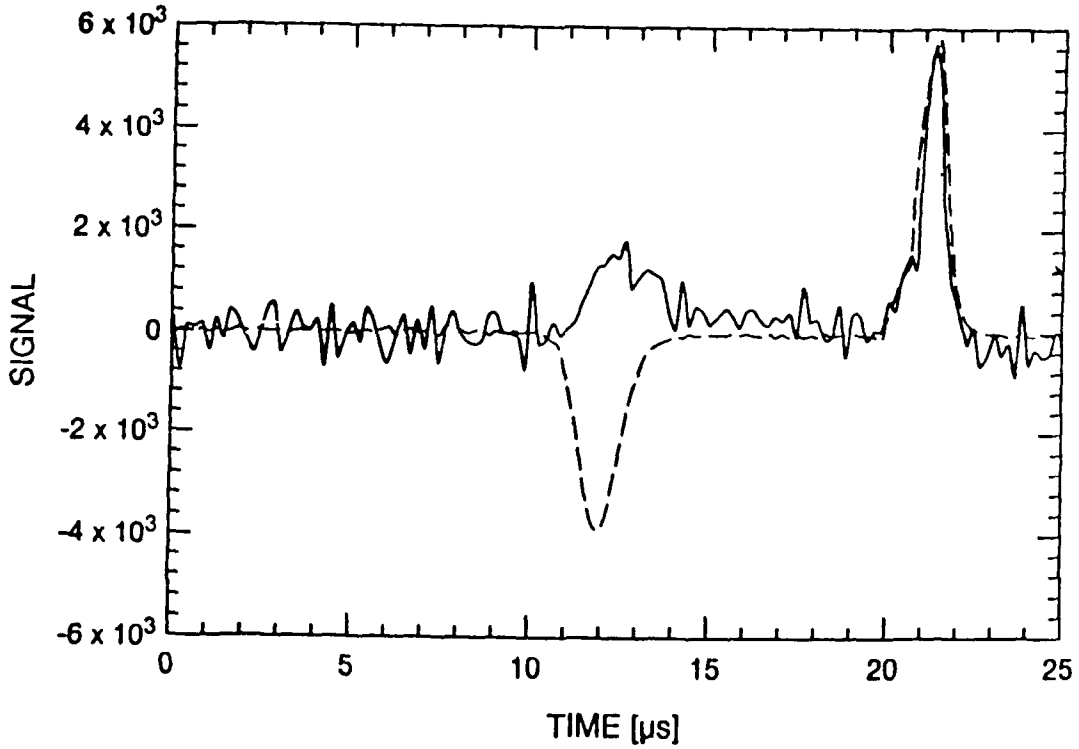

Figure 13. Derivatives of absorption transient and current showing the similarity of the duration of the time for relaxation of the ion velocity and of the current. The solid curve is calculated from the ion absorption and the dashed curve is calculated from the current.

B. Transient ion density.

In this section we demonstrate the utility of the laser absorption technique for measurements of the transient ion density and for determining the processes responsible for the loss of ions in the afterglow of a pulsed discharge. For these measurements of the N_2^+ density we measured absorption transients at the $A\ ^2\Pi_u \leftarrow X^2\Sigma_g^+$ (v'=2, v"=0) transitions of N_2^+ using the tunable diode laser operating near 790 nm. Once the ions cool to near the gas temperature, the absorption profile of the line is constant and the choice of laser frequency is not critical. If one wants to discuss absolute ion absorption coefficients, then one should measure the integrated line absorption. An absorption transient of N_2^+ is shown in Figure 14 for a pressure of 0.3 Torr.

The measured ion densities are such that losses due to dissociative recombination[26] of electrons with N_2^+, diffusion to the wall of the discharge tube[27], and ion conversion[28] are of comparable importance. Three-body recombination[29] and radiative recombination[30] are negligible compared to dissociative recombination for our conditions. Since an accurate model of spatially dependent decay of the N_2^+ density with all three loss processes active is very difficult to solve[31], we consider an approximate solution in which the spatially dependent diffusion term is replaced by the fundamental mode spatial solution. In this approximation, the N_2^+ density obeys the relation

$$\frac{dn_+}{dt} = -\alpha n_+ n_e - \frac{nD_a}{n\Lambda^2} n_+ - k_c n^2 n_+ ,$$

$$= -\alpha n_+^2 - \beta n_+ , \qquad (4)$$

where α is the recombination coefficient for N_2^+ and e, n_+ and n_e are the N_2^+ and electron densities, nD_a is the ambipolar diffusion coefficient at unit density, $\Lambda \equiv R/2.405$ is the fundamental mode diffusion length, k_c is the three-body rate coefficient for conversion of N_2^+ to N_4^+, and $\beta \equiv (nD_a)/n\Lambda^2 + kn^2$. In the limit of low electric fields such that the ions are in thermal equilibrium with the gas, ambipolar diffusion theory[27] shows that $nD_a = 2\ nD_+ = 2\ (kT/e)\ n\mu_+$, where nD_+ and $n\mu_+$ are the normalized diffusion and mobility coefficients for N_2^+ in N_2 and kT/e is the gas temperature in eV. In the final form of Equation (4), we assume $n_+ = n_e$. The errors resulting from the use of the simplified form of the diffusion term in Equation (4) have been discussed in by Frommhold and Biondi.[31] Also, the assumption that $n_+ = n_e$ is valid only so long as the density of N_2^+ is much greater than the density of N_4^+.

The solution to Equation (4) in the limit of very large τ, i.e., small loss by diffusion and ion conversion, is

$$\frac{1}{n_+} = \frac{1}{n_+(0)} + \frac{\alpha}{\beta}\left[e^{-\beta t} - 1 \right] , \qquad (5)$$

where $n_+(0)$ is the initial ion-electron density. The open points of Figure 14 show the excellent nonlinear least squares fit of Equation (5) to the experimental data. In the fitting procedure the decay constant β and the

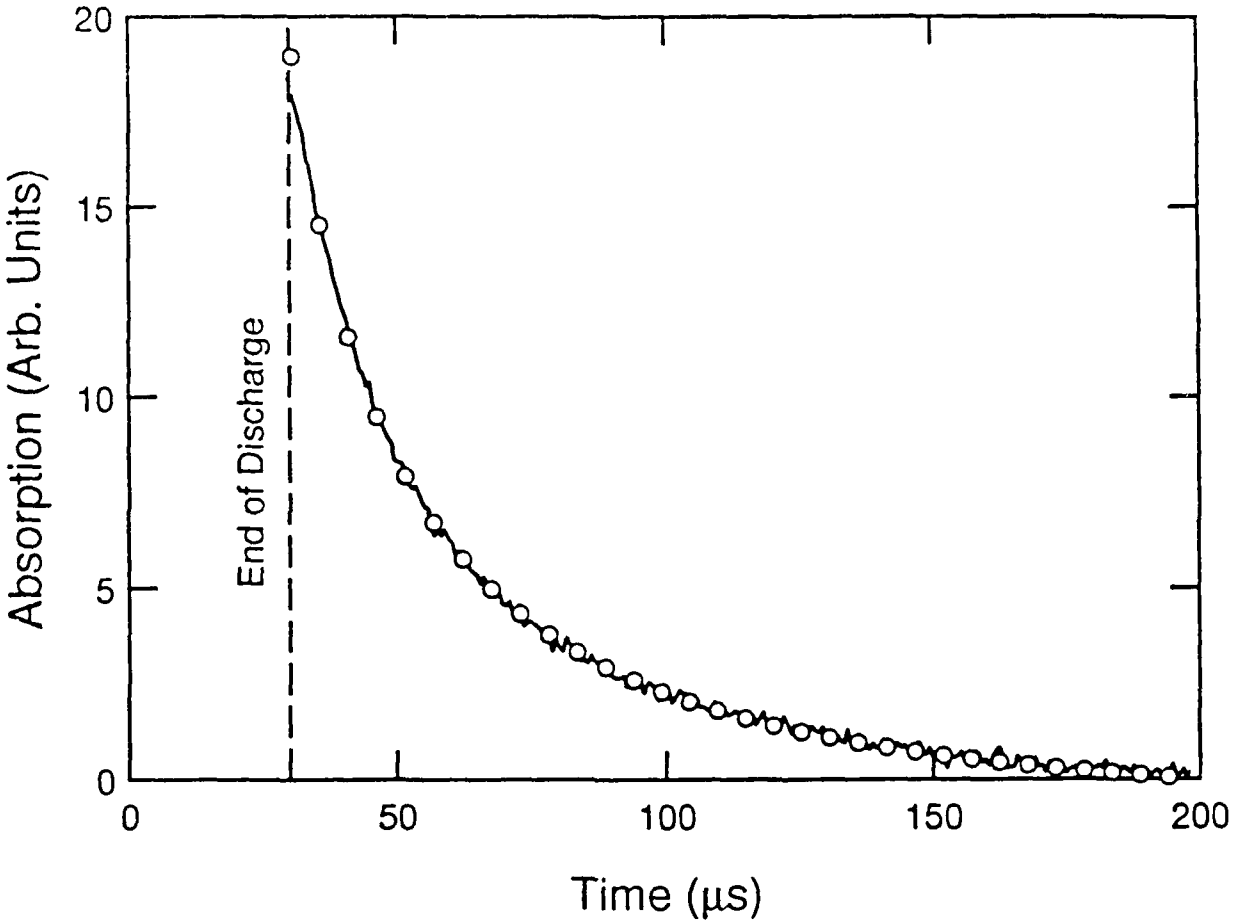

Figure 14. Transient absorption by N_2^+ showing ion density decay during the afterglow of the pulsed discharge. The points are a fit of Equation (5) to the experiment.

product of the recombination coefficient α and the initial ion density $n_+(0)$ were free parameters. The data of Figure 14 yield $\alpha n_+(0) = 4 \times 10^4\ s^{-1}$ and $\beta = 1.17 \times 10^4\ s^{-1}$. The average initial ion density $\langle n_+(0) \rangle$ calculated from the measured current and E/n value at the end of the discharge using data shown in Figure 6 is $5.3 \times 10^{17}\ m^{-3}$, so that of $\alpha = 8.2 \times 10^{-14}\ cm^3/s$. This recombination coefficient is significantly smaller than the value of $2.7 \times 10^{-7}\ cm^3/s$ measured in the afterglow of a microwave discharge[26] for 300 K electrons and ions. The value of β for 300 K ions and electrons calculated from $nD_a = 2.6 \times 10^{20}\ m^{-1}s^{-1}$ from ion drift velocity data[19] and $k_c = 4\text{-}8 \times 10^{-41}\ m^6/s$ from ion conversion measurements in drift tubes[28] is $5.6 \times 10^3\ s^{-1}$, with about equal contributions from diffusion and ion conversion. Thus, the apparent recombination coefficient is too small and the apparent diffusion plus ion conversion loss is too large. Both a small recombination coefficient and a large diffusion coefficient are consistent with the electron temperature being well above 300 K during the afterglow of our experiment. Evidence for the presence of an electric field which could heat the electrons during the afterglow was presented in Section IV.

The results presented in this section show that the laser absorption technique yields a very good signal to noise ratio and ion loss coefficients in rough agreement with published reaction coefficients describing the loss processes for N_2^+ in the afterglow of a pulsed discharge. We claim that with the advent of diode lasers the technique is much simpler to apply and is useful over a much greater range of experimental conditions than are, for example, the previously available techniques utilizing mass spectrometers for ion identification. The technique is presently limited to a few ions, such as N_2^+ and CO^+, which have absorption bands in the range of available lasers.

SECTION VI

INTERNAL ENERGY OF DRIFTING MOLECULAR IONS

Measurements of internal temperature of O_2^+ and N_2^+ ions drifting at elevated electric fields in helium have been carried out by Federer et al.[32] A more detailed study of vibrational excitation and quenching of N_2^+ in collision with He was presented later by Kriegel et al.[33] The rotational temperature of N_2^+ drifting in He was measured by Duncan et al.[34] All these drift tube experiments were performed in a buffer gas where charge transfer does not occur.

The present measurements are intended to test models for the gain of internal energy by molecular ions drifting through its parent gas where charge transfer is the dominant collision. In particular, we have measured the rotational populations of N_2^+ in a pulsed discharge in N_2 so as to test for rotational excitation as the result of collisions of the form

$$N_2^+(X\ ^2\Sigma_g^+,\ J') + N_2(X\ ^1\Sigma_g^+,\ J'') \rightarrow N_2^+(X\ ^2\Sigma_g^+,\ J''') + N_2(X\ ^1\Sigma_g^+,\ J'''').$$

The pulsed, high current discharge is used instead of a low current, steady-state drift tube in order to obtain a high enough ion density such that the laser absorption technique can be used. By using a short pulse of current and low energy input, the potentially interfering process resulting from gas heating, metastable state production, and vibrational excitation are kept small.

A. Experiment

The rotational population measurement was based on the relative integrated absorption for rotational transitions within the A $^2\Pi_u \leftarrow$ X $^2\Sigma_g^+$ (v'=2, v"=0) band. There were very few ion lines clearly separated from transitions of neutral nitrogen as shown in Figures 3 and 4. In order to obtain the integrated absorption for lines overlapped with transitions of N_2 we have fit the experimental profiles with sets of theoretical lineshapes. It is quite difficult to generate a set of asymmetric profiles because each frequency step required a numerical convolution as illustrated in Figure 10. To simplify the task we have used a multipass cell in which the laser beam was sent through the discharge cell in both directions, i.e., the laser was propagated from cathode to anode against the direction of drift of ions and was reflected back from anode to cathode along direction of the drift of ions. The first pass was seen by the drifting ions as shifted to the blue and the second pass was seen as shifted to the red. The resultant line shape was symmetrical. From the arguments of Section IV, the zero temperature absorption profiles were back-to-back half Gaussians and produced the effect of a full Gaussian with a width equal to twice that derived from Equation (2). Convolution of the thermal velocity profile produces a broader Gaussian profile. An experimental profile and its theoretical fit for the conditions of Figure 3 except for the change in the optical path is shown in Figure 15.

We were able to measure integrated absorption profiles of N_2^+ for rotational transitions for quantum numbers J as large as 20. Several of the N_2^+ transitions overlapped the First Positive band of N_2. An example is shown in Figure 16 where the ion line corresponding to the rotational quantum number J=14 is indicated by an arrow.

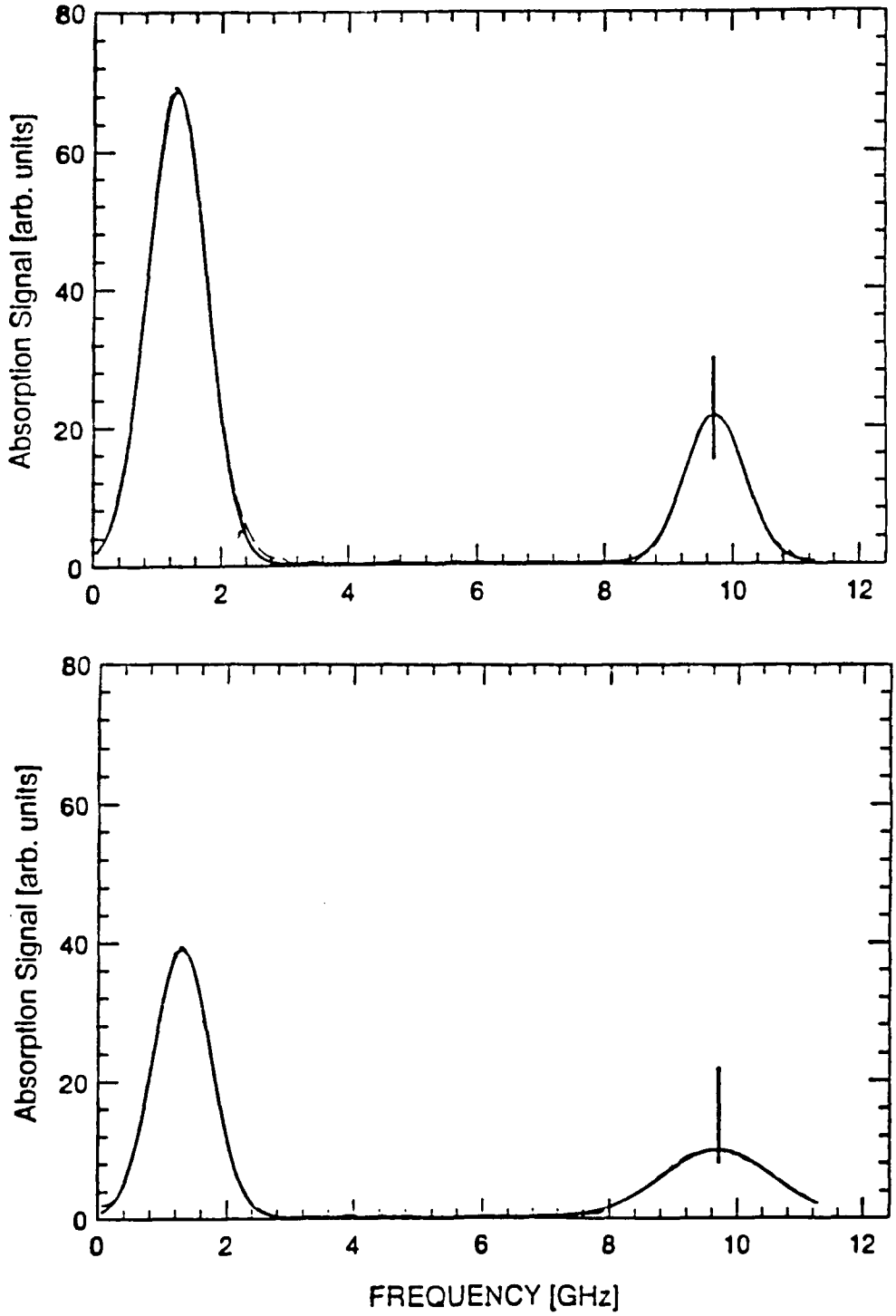

Figure 15. Absorption profiles for J' = 14 → J" = 12 transition. The lower profile was obtained during the discharge and the upper profile during the afterglow.

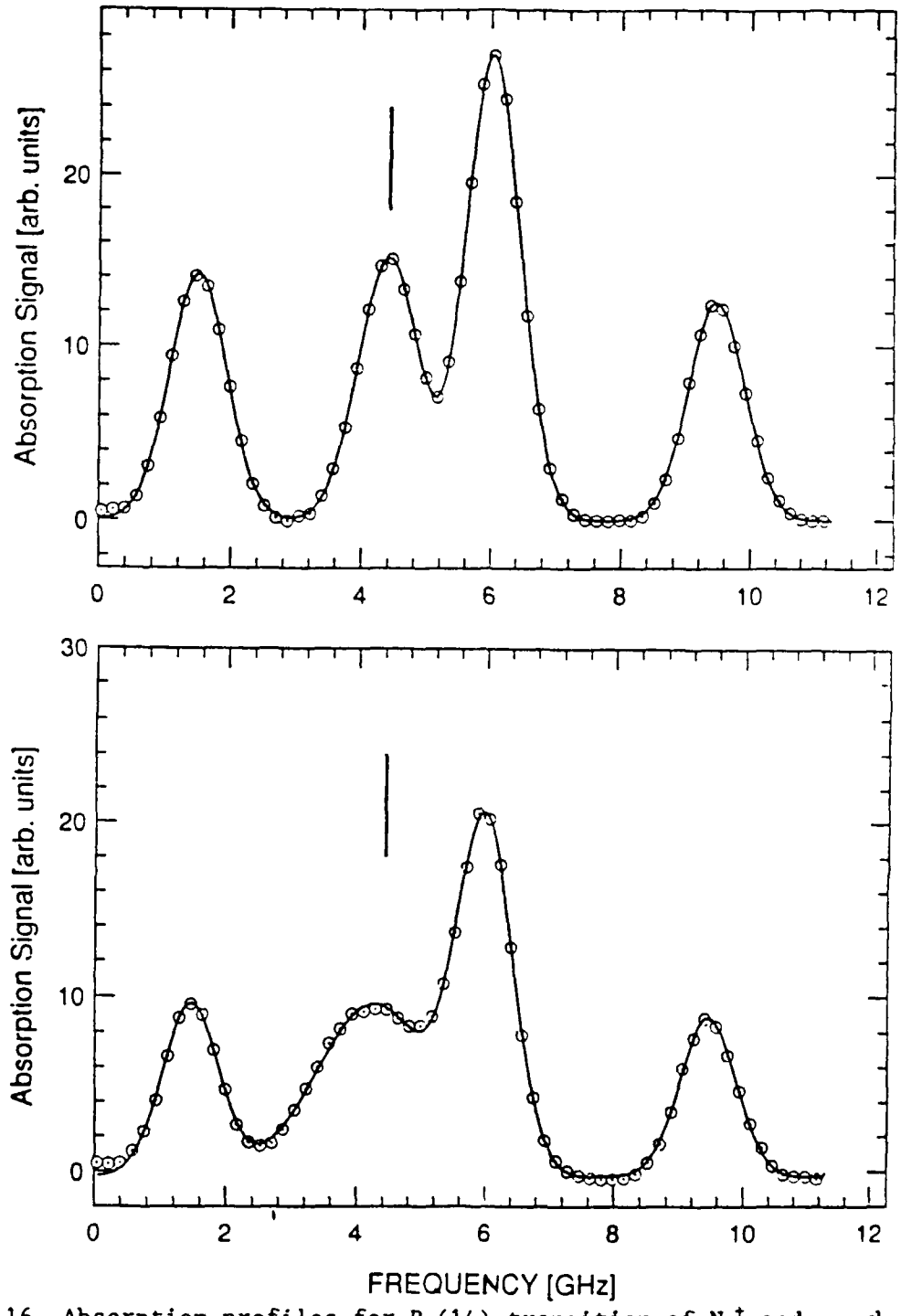

Figure 16. Absorption profiles for $R_1(14)$ transition of N_2^+ and nearby 1st positive showing bands showing fitting to data when interfering lines are present. The upper trace was obtained during the afterglow and the lower trace during the discharge. The points are experimental data and the curve is the result of the theoretical fit.

B. Rotational temperature determination.

The interpretation of the absorption intensities in terms of a rotational temperature requires a model which relates the intensities to the relative populations. Such models are available[35] for levels which are unperturbed by neighboring electronic states and for which the coupling between the spin and the angular momenta are simple. The X $^2\Sigma_g^+$ and A $^2\Pi_u$ involved in our absorption measurements are the ground and lowest electronically excited states of N_2^+. Since the vibrational levels of the transitions used in these experiments are well below the lowest vibrational level of the B $^2\Sigma_u^+$ state, the levels are not perturbed. The X $^2\Sigma$ state corresponds to pure Hund's case (b), while the B $^2\Sigma_u^+$ state is close to case (a).[36] The coupling schemes and absence of any perturbation was confirmed by Miller et al.[36] using laser induced fluorescence spectra of the A $^2\Pi_u \leftarrow$ X $^2\Sigma_g^+$ ($v' = 4 \leftarrow v'' = 0$) band. The Hönl-London factors are from Kovacs,[35] for Hund's case (b) and $\Delta\Lambda = 1$. Molecular constants for N_2^+ used for calculating the energy levels and partition function are from analyses of experimental spectra.[36-38]

For a Boltzmann distribution of rotational levels the relative absorption signals A(J) are given by

$$A(J) = \frac{A_0 \, S_J^R \, g_J}{Q(T_t, T_r)} \exp\left[- \frac{BJ(J+1)}{k \, T_r} \right] , \qquad (6)$$

where J is the rotational quantum number, $S_J^R = J + 2$, $Q(T_t, T_r)$ is partition function, T_t is the translational temperature of the gas, T_r is the rotational temperature of the N_2^+, g_J is the nuclear statistical factor of 1 for odd J and 2 for even J for N_2^+, and A_0 is a constant proportional to N_2^+ density.

A Boltzmann plot for a pure nitrogen discharge at a pressure of 0.3 Torr is shown in Figure 17. Integrated absorption signals normalized to $(J + 2)g_J$ are plotted for six rotational transitions during the discharge and in the afterglow. The rotational temperature is determined from the slope of the Boltzmann plot and Equation (6). We read for N_2^+ in N_2 a temperature equal to 350 ± 15 K and for N_2^+ in He, 430 ± 15 K during the discharge.

From the knowledge that the rotational distribution is well represented by the Boltzmann distribution, we have determined the rotational temperature for N_2^+ from the ratio of integrated intensities of the J = 20 line before and after the pulsed discharge for pressure up to 1.5 Torr.

C. Test of internal energy model.

Measurements of the vibrational temperature by Federer et al.[32] and Kriegel et al.[33] and of rotational temperature by Duncan et al.[34] for N_2^+ ions drifting through He were compared with theory by Viehland and Mason [39,40]. The measured internal temperature of the ions agreed very well with theory.

We have measured the rotational population distribution and temperature for N_2^+ in N_2, where charge transfer is dominant, and for N_2^+ drifting in He, where charge transfer is small. For nitrogen in helium discharge we have confirmed the measurements of the rotational temperature of N_2^+ drifting in He as measured by Duncan et al.[11] Our measurements are about five times more precise than those of reference 11.

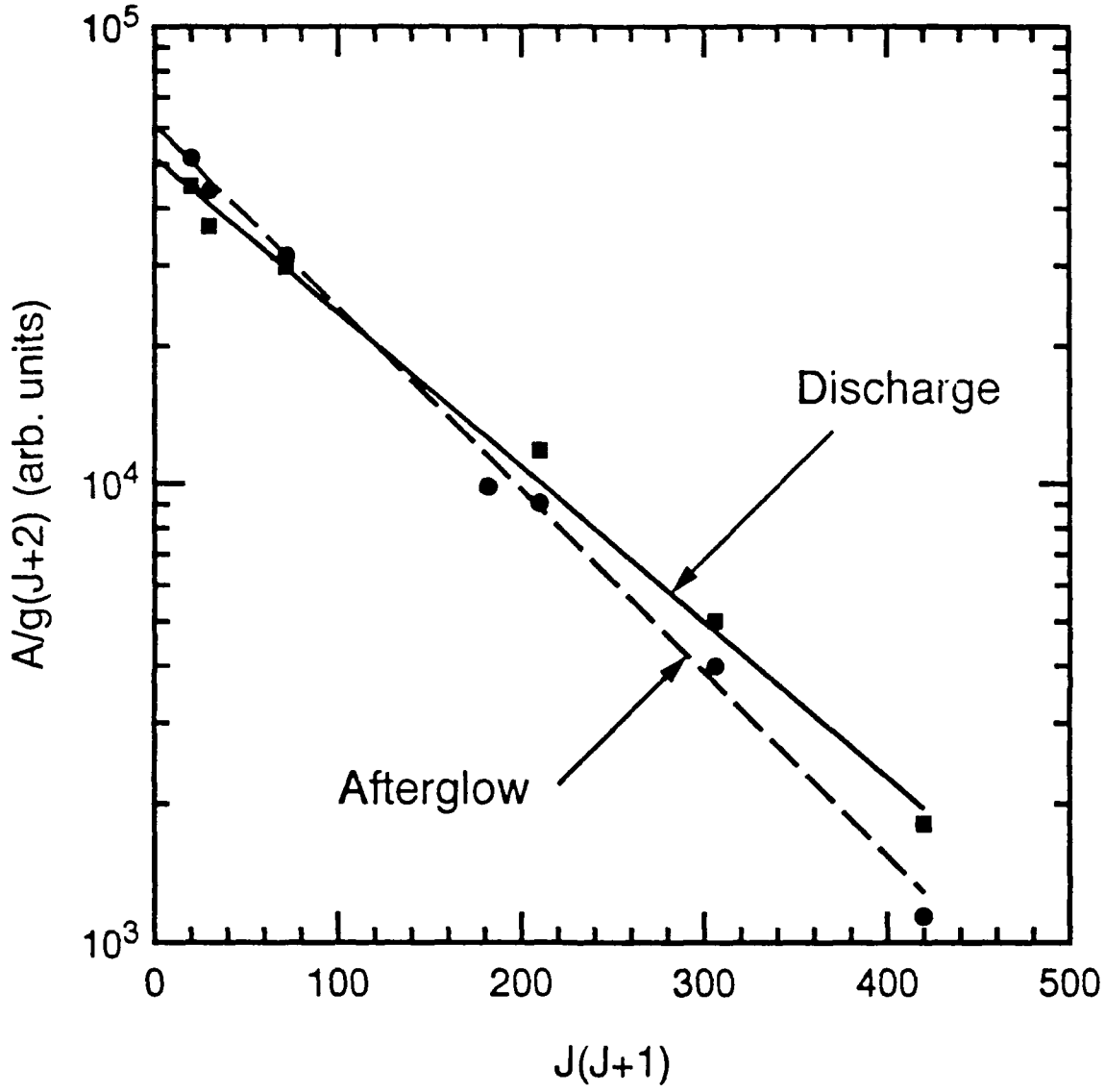

Figure 17. Boltzmann plot showing the rotational temperature during the discharge, solid line, and during the afterglow, dashed line.

According to Viehland, Lin, and Mason[40] as quoted by Kriegel et al.[33] the expression for the internal temperature T_i of a molecular ion drifting through an atomic buffer gas is

$$\frac{3}{2} k T_i = \left(1 + \xi \frac{M_b}{M_i} \right)^{-1} \frac{3}{2} k T_b + \frac{1}{2} M_b v_d^2 , \qquad (7)$$

where T_b is the temperature of the buffer gas, M_b is the mass of the buffer gas, M_i is the mass of an ion, ξ is the fractional energy loss per inelastic collision, v_d is the ion drift velocity, k is the Boltzmann constant.

The ion drift velocities were determined from the Doppler shifted and broadened absorption profiles of N_2^+ measured using the diode laser system. The results for 0.3 Torr pressure are given in Table 1. The uncertainty quoted is for repeated measurements within a short period of time and is limited by the stability of our laser system. However, the long term experimental reproducibility is lower for reasons that are not fully understood.

Table 1. Internal energy data for N_2^+ in N_2 and He.

Pressure = 0.3 Torr.

	N_2^+ in N_2	N_2^+ in He
E/n (Td)	125	16
p (Torr)	0.3	0.3
v_d (cm/s)	$4.8 \pm 0.8 \times 10^4$	$8.8 \pm 0.8 \times 10^4$
T_i Theory	407 K	418 K
T_i Exp.	350 ± 15 K	430 ± 15 K

In the case of a pure nitrogen discharge, the temperature T_b of the N_2 was obtained from observation of the Doppler width of a ro-vibrational absorption line of the First Positive band of neutral nitrogen $B\ ^3\Pi_g \leftarrow A\ ^3\Sigma_u$ ($v'=7 \leftarrow v''=6$). The derived temperature was $T_b = 293 \pm 5$ K. For the nitrogen-helium mixture we have assumed that the translational temperature of the buffer gas T_b is equal to 300 K. We did not monitor any N_2 transitions in the N_2 - He experiments and so did not check for a temperature rise. The calculated rise in the He temperature is small because of the low electric field.

A lower limit to the theoretical internal temperature of N_2^+ drifting in N_2 of $T_i = 407$ K is obtained from Equation (7) using $\xi = 1$. This value of ϵ is equivalent to the conventional assumption that all the internal energy is lost to the N_2 in charge transfer collisions.[21,22] However, a value of $\epsilon \approx 2$ would be required to reduce the calculated value of T_i to the experimental value of 350 K. We conclude that for N_2^+ in N_2 the present form Equation (7) is not applicable. It remains to be seen how one can quantitatively relate the experimentally significant increase in internal temperature for N_2^+ in N_2 to the expected[41] rapid rise in the cross section for rotational excitation near threshold and to the prediction[41] that the cross section for vibrational excitation is about 10 percent of the charge transfer cross section at ion energies from 1 eV to 100 eV.

The internal temperature calculated using Equation (7) for N_2^+ in He and the conditions of Table 1 is $T_i = 418$ K for $\xi = 0$. Using $\xi = 0$ is equivalent to the assumption that the inelastic energy loss in collisions of N_2^+ with helium is negligible, i.e., that the cross sections for rotational and

vibrational excitation and deexcitation are small. This result agrees well with our experiment. This agreement is consistent with other researchers.[34]

SECTION VII

IMPACT OF MEASUREMENTS OF METASTABLE PROPERTIES

This section is concerned with the impact of measurements made under this program on models of the production of ionization in high current discharges in N_2. In particular, we will estimate the relative contributions of ionization by collisions between various pairs of excited states of N_2 for representative discharge conditions. The excited state pairs under consideration include an N_2 in one of the A $^3\Sigma_u^+$, a' $^1\Sigma_u^-$, and a" $^1\Sigma_g^+$ metastable states of N_2 and an N_2 molecule in one of the various vibrational levels of the X $^1\Sigma_g^+$ ground state. In addition, we consider various combinations of molecules excited to metastable and radiating states. Associative ionization in collisions of pairs of these molecules have been proposed[42-47] as being responsible for the growth of ionization instabilities in high power, electric discharge lasers utilizing N_2. The pairs under consideration and the corresponding rate coefficients are listed in Table 2. In each case involving the X $^1\Sigma_g^+$ ground state, the vibrational level of the X state is chosen such that the sum of the excitation energies ϵ_1 for state 1 and ϵ_2 for state 2 is just greater than the ionization potential of N_2 of 15.58 eV or the energy necessary to form N_{4+} by associative ionization of 14.63 eV. Although associative ionization in collisions of excited N_2 with N_2 in the ground vibrational state to form N_{4+} is improbable,[48] associative ionization is favored in most[49,50], but not all,[51,52] recent models of high current discharges in N_2. In Tables 3 and 4

Table 2. Excited state pairs considered as sources of ionization in N_2. Rate coefficients for quenching, electron excitation at E/n = 100 Td, and associative ionization.

Pair	State 1	State 2	ϵ_1 eV	ϵ_2 eV	k_1 m^3/s	Ref.	$k_{eX}{}^1$ m^3/s	Ref.	k_{AI} m^3/s	Ref.
X X	$X^1\Sigma_g^+(v=32)$	$X^1\Sigma_g^+(v=32)$	7.8	7.8	NA[a]		NA		1(-19)	49
A X	$A^3\Sigma_u^+(v=0)$	$X^1\Sigma_g^+(v\approx35)$	6.17	8.46	2.6(-24)[b]	53	1.4(-17)	11	1(-19)	49
a'X	$a'^1\Sigma_u^-(v=0)$	$X^1\Sigma_g^+(v=26)$	8.40	6.23	2.2(-19)	54	5.0(-19)	11	1(-19)	49
C X	$C^3\Pi_u(v=0)$	$X^1\Sigma_g^+(v=14)$	11.03	3.60	2(-17)	55	1.0(-18)	11	1(-19)	49
E X	$E^3\Sigma_g^+(v=0)$	$X^1\Sigma_g^+(v=10)$	11.88	2.75	1(-16)	56	1.0(-19)	11	1(-19)	49
a"X	$a''^1\Sigma_g^+(v=0)$	$X^1\Sigma_g^+(v=9)$	12.26	2.37	3(-16)	10	1.0(-19)	11	1(-19)	49
a'A	$a'^1\Sigma_u^-(v=0)$	$A^3\Sigma_u^+(v=0)$	8.40	6.17	2.2(-19)	54	5.0(-19)	11	6(-18)	46
a'a'	$a'^1\Sigma_u^-(v=0)$	$a'^1\Sigma_u^-(v=0)$	8.40	8.40	2.2(-19)	54	5.0(-19)	11	6(-18)	46
C A	$C^3\Pi_u(v=0)$	$A^3\Sigma_u^+(v=0)$	11.03	6.17	2(-17)	55	1.0(-18)	11	6(-18)	46
C a'	$C^3\Pi_u(v=0)$	$a'^1\Sigma_u^-(v=0)$	11.03	8.40	2(-17)	55	1.0(-18)	11	6(-18)	46
a"A	$a''^1\Sigma_g^+(v=0)$	$A^3\Sigma_u^+(v=0)$	12.26	2.37	3(-16)	10	1.0(-19)	11	6(-18)	46

[a] NA means that the use of a quenching rate coefficient is inappropriate. See text.

[b] 2.6(-18) means 2.6×10^{-18}

we have estimated fractional populations and the contributions of various processes to the ionization rate for two very different discharge conditions. The conditions for Table 3 are those used by Capitelli, Dilonardo, and Gorse[50] and approximate those of a high pressure discharge in N_2 operating at power levels similar to those of a CO_2 laser. The conditions for Table 4 are adjusted to approximate those at the end of the pulsed discharge used in our experiments.

The importance of ionization by N_4^+ formation by the X X pair has been advocated to explain the measured nonlinear dependence of the ionization rate on the degree of ionization of the N_2.[42,45,50] One reason for considering this pair is that in a high current electrical discharge the populations of the higher vibrational levels of the X state are known to be far in excess of those calculated from a Boltzmann distribution at the "temperature" of the lower vibrational levels. This excess is attributed to anharmonic pumping.[50,53] In Table 3 we have taken the fractional populations of the vibrational levels of the X state from the calculations of Capitelli, Dilonardo, and Gorse.[50] In Table 4 we have calculated the vibrational populations from the rise in vibrational temperature under the assumption that essentially all of the energy input is to vibrational excitation[3] and that vibrational relaxation[49] occurs on a time scale short compared to the length of the pulsed discharge. The rate coefficient listed in Table 2 for associative ionization in X X collisions is taken from Capitelli, Dilonardo, and Gorse.[50]

Associative ionization of the a"X pair has been advocated by several authors[42,45] as an important source of ionization responsible for the growth of instabilities in N_2 discharges. As discussed in AFWAL-TR-88-2033, we have

Table 3. Estimates of ionization by various collision processes in a steady-state N_2 discharge for $n_e = 10^{19}$ m^{-3}, $n = 10^{25}$ m^{-3}, and E/n = 60 Td. Note that the electron excitation coefficients used are those for E/n = 100 Td as an approximate allowance for the effects of vibrational excitation.

Pair	[n1]/n[a]	[n2]/n	$f(T_v,v)$	$R_{AI}(1,2)/R_{eI}$
X X	NA[b]	NA	2.3(-2)	1.8(4)
A X	4.6(-4)[c]	NA	2(-2)	3.1(2)
a'X	1.4(-4)	NA	3(-2)	1.4(2)
C X	2.1(-6)	NA	6(-2)	4.3
E X	1.3(-8)	NA	1(-1)	4.3(-2)
a"X	2.3(-9)	NA	1(-1)	7.8(-3)
a'A	1.4(-4)	4.6(-4)	NA	1.4(2)
a'a'	4.6(-4)	1.4(-4)	NA	4.2(1)
C A	2.1(-6)	4.6(-4)	NA	2.0
C a'	2.1(-6)	1.4(-4)	NA	6.2(-1)
a"A	2.3(-9)	4.6(-4)	NA	2.2(-3)
e A	1.0(-6)	4.6(-4)	NA	1.6(-1)

[a] [n1] means density of the first of the excited state pair listed in column 1, while [n2] is the density of the second of the excited state pair.

[b] NA means not applicable.

[b] 2.6(-18) means 2.6×10^{-18}.

Table 4. Estimates of ionization by various collision processes at the end of a pulsed N_2 discharge for $n_e = 3.8 \times 10^{17}$ m^{-3}, $n = 10^{22}$ m^{-3}, and E/n = 100 Td.

Pair	[n1]/n[a]	[n2]/n	$f(T_v,v)$	$R_{AI}(1,2)/R_{eI}$
X X	NA[b]	NA	4.2(-63)	-
A X	1.1(-3)[c]	NA	2.2(-68)	7.9(-64)
a'X	3.8(-3)	NA	1.5(-50)	1.9(-45)
C X	6.2(-7)	NA	1.6(-29)	3.4(-28)
E X	4.9(-7)	NA	1.0(-22)	1.7(-21)
a"X	8.9(-8)	NA	1.1(-19)	3.3(-19)
a'A	3.8(-3)	1.1(-3)	NA	1.6
a'a'	3.8(-3)	3.8(-3)	NA	5.7
C A	6.2(-7)	1.1(-3)	NA	2.6(-4)
C a'	6.2(-7)	3.8(-3)	NA	9.2(-4)
a"A	8.9(-8)	1.1(-3)	NA	3.7(-5)
e A	3.8(-5)	1.1(-3)	NA	2.7(-1)

a [n1] means density of the first of the excited state pair listed in column 1, while [n2] is the density of the second of the excited state pair.

[b] NA means not applicable.

[b] 2.6(-18) means 2.6×10^{-18}.

used the laser absorption technique to measure the lifetimes of the a" state and to determine rate coefficients for collisional coupling among the rotational levels of the lowest vibrational state and for collisional quenching to lower electronic states. The measurements make possible for the first time the evaluation of the a"X associative ionization process as a source of electrons in N_2 discharges. Our quenching coefficient for the a" state is listed in Table 2.

We will use the a" state kinetics to illustrate the calculation of the contribution of metastable states to the nonlinear growth of ionization in N_2 discharges. The rate equation governing the a" $^1\Sigma_g^+(v = 0)$ density [a"] is

$$\frac{d[a"]}{dt} = k_e(a") \; n \; n_e - k_q(a") \; n \; [a"] - A(a") \; [a"] \; , \qquad (8)$$

where $k_e(a")$ is the rate coefficient for electron excitation of N_2 to the a" state, $k_q(a")$ is the rate coefficient for quenching of the a" state to a lower electronic level, n_e is the electron density, and $A(a")$ is the radiative lifetime of the a" state. Here the destruction of the a" in collisions with the vibrationally excited X state or with other electronically excited states has been neglected. The steady-state solution to Equation (8) is

$$[a"] = \frac{k_e(a") \; n_e \; n}{k_q(a") \; n + A} \; . \qquad (9)$$

Note that since the radiative lifetime for the a" state is very long, the denominator of Equation (9) is approximately k_q n and the N_2 density cancels out of the result. In general, it is convenient to divide both sides of

Equation (9) by the gas density n and express the result as in Tables 2 and 3. The rate of associative ionization is given by

$$R_{AI}(a''X) = k_{AI}(a''X)\ [a'']\ [X(v > 13)]$$

$$= k_{AI}(a''X)\ f(T_v,13)\ n\ \frac{k_e(a'')\ n_e\ n}{k_q(a'')\ n + A} \quad . \qquad (10)$$

Here $k_{AI}(a''X)$ is rate coefficient for associative ionization rate in collision between N_2 molecules in the a" state and vibrationally excited N_2 with $v > 13$ and $f(T_v,13)$ is the fraction of the N_2 molecules with $v > 13$. The fraction $f(T_v,v)$, where v is the lowest vibrational level capable of supplying the energy required for associative ionization, is obtained from theoretical calculations.[50,53]

Since the rate of ionization in collision between electrons and N_2 is $R_{eI} = k_{eI}\ n\ n_e$, the ratio of associative ionization to direct or single step ionization is

$$\frac{R_{AI}(a''X)}{R_{eI}} = \frac{k_{AI}(a''X)\ f(T_v,\ 13)\ k_e(a'')\ n}{k_q(a'')\ n\ +\ A} \quad . \qquad (11)$$

In order to complete the prediction of the importance of this process, we must estimate the effect of the population of high vibrational levels of the X state on the rate coefficients for electron excitation of the a" state. In Table 3 we have approximated the results[50] of models of discharges in N_2 by raising the effective E/n to 100 Td. This procedure gets around the absence of published results for excited states of interest. Equation (11) is easily

modified by inspection for use in calculating the ratios of ionization rates appropriate to associative ionization in collisions of other electronically excited states of N_2 and vibrationally excited, ground state N_2. The results are given in Tables 3 and 4.

The rate of associative ionization collisions involving electronically excited N_2 in the a' $^1\Sigma_u^-(v = 0)$ and A $^3\Sigma_u^+(v = 0)$ states is given by

$$R_{AI}(a"A) = k_{AI}(a"A)\,[a"]\,[A]$$

$$= k_{AI}(a"A)\,\frac{k_e(a")\,n_e\,n}{k_q(a")n + A(a")_q} \times \frac{k_e(A)\,n_e\,n}{k_q(A)n + A(A)} \quad . \qquad (12)$$

Here $k_{AI}(a"A)$ is the rate coefficient for associative ionization rate in collision between N_2 molecules in the a" and A states. The corresponding ratio of the rate of associative ionization for the a" and A states to that for electron impact ionization is

$$\frac{R_{AI}(a"A)}{R_{eI}} = \frac{k_{AI}(a"A)\,k_e(a")\,k_e(A)\,n^2}{\left[k_q(a")\,n + A(a")\right]\left[k_q(A)n + A(A)\right]} \quad . \qquad (13)$$

Values of the ratio given by Equation (13) for steady-state and pulsed discharges are given in Tables 4 and 5. Again, Equation (13) is easily modified by inspection for use in calculating the ratios of ionization rates appropriate to associative ionization in collisions of other pairs of electronically excited states of N_2.

The results of the calculations presented in Table 3 illustrate the potential importance of ionization resulting from collisions involving N_2 molecules in high vibrational states. Thus, if the rate coefficient for associative ionization in collisions between pairs of X $^1\Sigma_g^+(v = 32)$

corresponded to an average cross section of only 10^{-26} m^2 or 10^{-22} cm^2, this ionization process would compete with single-step ionization of N_2 by electron impact. A significant contribution from associative ionization involving electronically excited N_2 and vibrationally excited N_2 would require much larger rate coefficients. Although it is impossible to rule out such a small associative ionization cross section, present opinion[44,46,47] is that the X X process is not important. The skepticism concerning the rate coefficient for the X X ionization process is based on the expected difficulty of converting large amounts of vibrational energy ($v = 32$) into the electronic energy required for ionization, i.e., the expected low probability for a favorable curve crossing between the product N_4^+ in its ground vibrational state and the wildly vibrating N_4 formed from two highly excited N_2 molecules.

The calculations presented in Table 4 suggest to us the possibility that by using a pulsed discharge one could measure the rate coefficient for associative ionization from the a'A or a'a' pairs without the complications resulting from high populations of vibrationally excited N_2. The suggestion that collisions between pairs of N_2 molecules in the a' state may be responsible for the growth of ionization instabilities was made some time ago by Brunet, Vincent, and Rocca-Serra.[44] As yet there has been no direct measurement of associative ionization rate coefficients for excited N_2. A possible means of producing a' state molecules, without the complications of electrons produced by a discharge, is by two-photon absorption to the a state[55,58] and subsequent collisional relaxation to the a' state.[55]

SECTION VIII

CONCLUSIONS

In our study of the behavior of molecular ions in the positive column in the low pressure gas discharge, we have demonstrated that an analysis of the absorption line shape is a good method for measuring a macroscopic electric field in N_2 discharges. We claim the accuracy of the measurements of drift velocity to be a few percent so that the accuracy of the E/n determination is comparable with the accuracy of the published measurements of N_2^+ drift velocity versus E/n. Additionally, we have shown that when the contribution to the velocity of the ions from the electric field is comparable with the thermal velocity, the convolution of the high field velocity distribution and the thermal Maxwellian distribution satisfactorily represents the velocity distribution. We have demonstrated that for N_2^+ in N_2 there is no dependence of the drift velocity on the rotational state of an ion. We also have shown that the rotational population of the N_2^+ follows closely the Boltzmann distribution and we have measured the rotational temperature of N_2^+. We have found good agreement of measured rotational temperature with the results of widely used theory of Viehland et al. for N_2^+ drifting in He as buffer gas. The same theory fails to predict the internal temperature of N_2^+ drifting in N_2 where the charge transfer plays a significant role in the collisional process.

Advantages of the laser absorption-Doppler shift method for determination of the E/n presented in this report are that the method is nonintrusive and that time resolution on the microsecond scale can be obtained. The method also makes possible accurate translational temperature

determinations of the gas with a high time resolution during the discharge and afterglow.

Recommendations for future work are:

(1) Use the diode laser absorption technique to measure the N_2^+ spatial and time dependence in the cathode fall region of moderate current discharges in N_2. The absorption technique and the associated laser induced fluorescence are much more quantitative than the optogalvanic technique used for N_2^+ thus far.[59]

(2) Measure the time dependent E/n and ion densities during the build up of the discharge current so as to test recently developed models.[60]

(3) Extend the absorption technique to lower vibrational levels of the $A^2\Pi_u$ state using the newly available diode lasers operating near 810 nm.

(4) Extend the absorption technique to the v = 1 vibrational level of the X $^2\Sigma_u^+$ state using diode lasers operating near 810 nm so as to search for vibrational excitation of the N_2^+. Not only does this test the theories of internal energy of drifting ions,[24] but it should yield information regarding the important process[61] of dissociation of N_2^+ at high E/n.

(5) As shorter wavelength diodes become available, the absorption technique should be extended to other gaseous ions, e.g., CO^+ at $\approx$ 500 nm.

(6) Use absorption by N_2^+ as a probe of the electric field in discharges seeded with small additions of N_2.

(7) Use simultaneous measurements of the N_2^+ and metastable densities by laser absorption and of the electron density by microwave techniques to determine the role of associative ionization in the growth of electron density at high current densities.

(8) Use the pulsed positive column discharge with laser diode diagnostics to separate two-stage ionization involving relatively short lived electronically excited states, such as the a' state, from two-stage ionization involving long lived species, such as vibrationally excited N_2. This same approach would separate out proposed [46] three-stage ionization involving N_2 metastables in the A-state or vibrationally-excited, X-state molecules.

(9) Look for laser absorption by N_4^+ at wavelengths in the vicinity of 390 nm. A diagnostic for this ion would be very useful in determining the importance of associative ionization in N_2 discharges.

REFERENCES

1. B.N. Ganguly and A. Garscadden, Phys. Rev. A 32, 2544 (1985); B.N. Ganguly J. Appl. Phys. 60, 571 (1986); B.N. Ganguly, J.R. Schoemaker, B.L. Preppernau, and A. Garscadden, J. Appl. Phys. 61, 2778 (1987); J.R. Shoemaker, B.N. Ganguly, and A. Garscadden, Appl. Phys. Lett. 52, 2019 (1988).

2. N. Laegreid and G.K. Wehner, J. Appl. Phys. 32, 365 (1961).

3. A.G. Engelhardt, A.V. Phelps, and C.G. Risk, Phys. Rev. 135, A1566 (1964).

4. K.M. Evenson and D.S. Burch, J. Chem. Phys. 45, 2450 (1966).

5. A.B. Wedding and A.V. Phelps, J. Chem. Phys. 89, 2965 (1988).

6. J.L. Hall and S.A. Lee, Appl. Phys. Lett. 29, 367 (1976).

7. A. Lofthus and P.H. Krupenie, J. Phys. Chem. Ref. Data 6, 113 (1977).

8. G.H. Dieke and D.F. Heath, Johns Hopkins Spectroscopic Report No. 17, 1959 (unpublished). We thank W. Benesh for a copy of relevant portions of this table.

9. M.J. Druyvesteyn and F.M. Penning, Rev Mod. Phys. 12, 87 (1940).

10. A.B. Wedding, J. Borysow, and A.V. Phelps (unpublished).

11. A.V. Phelps and L.C. Pitchford, Phys. Rev. 31, 2932 (1985); A.V. Phelps and L.C. Pitchford, JILA Data Center Report No. 26, May 1985 (unpublished).

12. J.F. Waymouth, J. Appl. Phys. 37, 4492 (1966).

13. C. Wieman and T.W. Hansch, Phys. Rev. Letters 36, 1170 (1976).

14. D.K. Doughty and J.E. Lawler, Appl. Phys. Lett. 45, 611 (1984); D.K. Doughty, S. Salih, and J.E. Lawler, Phys. Lett. 103A, 41 (1984).

15. C.A. Moore, G.P. Davis, and R.A. Gottscho, Phys. Rev. Lett. 52, 538 (1984); R.A. Gottscho, Phys. Rev. A 36, 2233 (1987).

16. J. Derouard and N. Sadeghi, IEEE Trans. Plasma Science PS-14, 515 (1986); H.Debontride, J. Derouard, P. Edel, R. Romestain, N. Sadeghi, and J.P. Boeuf, Phys. Rev. A 40, 5208 (1989).

17. N.N. Haese, F.-S. Pan, and T. Oka, Phys. Rev. Lett. 50, 1575 (1983).

18. M.B. Radunsky and R.J. Saykally, Chem. Phys. Lett. 152, 419 (1988).

19. H.W. Ellis, R. Y. Pai, E.W. McDaniel, E.A. Mason, and L.A. Viehland, Atomic Data and Nuclear Data Tables 17, 177 (1976).

20. C.H. Muller, Jr. and A.V. Phelps, J. Appl. Phys. 51, 6141 (1980).

21. G. H. Wannier, Statistical Physics, (Wiley, New York, 1966).

22. J.E. Lawler, Phys. Rev. 32, 2977 (1985).

23. Ch.S. Gudeman, C.C. Martner, and R.J. Saykally, Chem. Phys. Lett. 122, 108 (1985).

24. L.A. Vieland, S.L. Lin, and E.A. Mason Chem. Phys. 54, 341 (1981).

25. R.A. Dressler, J.P.M. Beijers, H. Meyer, S.M. Penn, V.M. Bierbaum, and S.R. Leone, J. Chem. Phys. 89, 4707 (1988).

26. M.A. Biondi, in Principles of Laser Plasmas, Edited by G. Bekefi (Wiley, New York, 1976), Chap. 4; P.M. Mul and J.Wm. McGowan, J. Phys. B 12, 1591 (1979).

27. H.J. Oskam, Phillips Res. Repts. 13, 335 (1958).

28. T.D. Märk, Int. Jour. Mass Spectrom. and Ion Phys. 9, 387 (1972).

29. D.R. Bates, in Case Studies in Atomic Physics, Edited by M.R.C. McDowell and E.W. McDaniel (North-Holland, Amsterdam, 1973); D.R. Bates, J. Phys. B 13, 2587 (1980).

30. J. Bacri and A.M. Gomes, J. Phys. D 19, 1665 (1986).

31. L. Frommhold and M. A. Biondi, Annals of Physics, 48, 407 (1968).

32. W. Federer, H. Ramler, H. Villinger, and W. Lindinger, Phys. Rev. Lett. 54, 540 (1984).

33. M. Kriegel, R. Richter, W. Lindinger, L. Barbier, and E.E. Ferguson, J. Chem. Phys. 88, 213 (1988).

34. M.A. Duncan, V.M. Bierbaum, G.B. Ellison, and S.R. Leone, J. Chem. Phys. 79, 5448 (1984).

35. I. Kovacs, Rotational Structure in the Spectra of Diatomic Molecules (American Elsevier, New York, 1969) p.123.

36. T.A. Miller, T.Suzuki, and E. Hirota, J. Chem. Phys. 80, 4671 (1984).

37. A.E. Douglas, Astrophys. J. 117, 380 (1953).

38. J.C. Hansen, C.H. Kuo, F.J. Grieman, and J.T. Moseley, J. Chem. Phys.79, 1111 (1983).

39. L.A. Viehland and E.A. Mason, Ann. Phys.(N.Y.) 110, 287 (1978); S.L. Lin, L.A. Viehland and E.A. Mason, Chem. Phys. 37, 411 (1979).

40. L.A. Viehland, S.L. Lin and E.A. Mason, Chem. Phys. 54, 341 (1981); L.A. Viehland and R.E. Robson, Int. J. Mass Spectrom. Ion Processes 90, 167 (1989).

41. A.V. Phelps, J. Phys. Chem. Ref. Data (submitted) (1990); T.F. Moran, K.J. McCann, and M.R. Flannery, 63, 3857 (1975).

42. I.S. Polak, P.A. Sergeev, and D.I. Slovetskii, Teplofiz. Vys. Temp. 15, 15 (1977); [High Temperature 15, 13 (1977)].

43. O.V. Achasov, S.A. Zhdanok, D.S. Ragozin, R.I. Soloukhin, and N.A. Fomin, Zh. Eksp. Teor. Fiz. 81, 550 (1981); [Sov. Phys. JEPT, 54, 294 (1981)].

44. H. Brunet, P. Vincent, and J. Rocca-Serra, J. Appl. Phys. 54, 4951 (1983); H. Brunet and J. Rocca-Serra, J. Appl. Phys. 57, 1574 (1985).

45. Yu.B. Golubovskii and V.M. Telezhko, Teplofiz. Vys. Temp. 22, 428 (1984); [High Temperature 22, 340 (1984)].

46. K.V. Baiadze, V.M. Vetsko, G.B. Lopantseva, A.P. Narpartovich, A.F. Pal', A.V. Perevoznov, T.E. Popova, A.N. Starostin, and A.V. Filippov, Fiz. Plasmy 11, 352 (1985); [Sov. J. Plasma Phys. 11, 205 (1985)].

47. A.V. Berdyshev, I.V. Kochetov, and A.P. Napartovich, Fiz. Plasmy. 14, 741 (1988); [Sov. J. Plasma Phys. 14, 438 (1988)].

48. R.K. Asundi, G.J. Schulz, and P.J. Chantry, J. Chem. Phys. 47, 1584 (1967).

49. J. Loureiro and C.M. Ferreira, J. Phys. D 19, 17 (1989); 22, 67 (1989).

50. M. Capitelli, M. Dilonardo, and G. Gorse, Chem. Phys. 56, 29 (1981); M. Cacciatore, M. Capitelli, and C. Gorse, Chem. Phys. 66, 141 (1982).

51. J.P. Boeuf and E.E. Kunhardt, J. Appl. Phys. 60, 915 (1986).

52. S.K. Dahli and L.H. Low, J. Appl. Phys. 64, 2917 (1989).

53. B.F. Gordiets, A.L. Osipov, E.V. Stupochenko, and L.A. Sheplin, Usp. Fiz. Nauk 108, 655 (1973); [Soviet Phys. Uspeki 15, 759 (1973)].

54. D. Levron and A.V. Phelps, J. Chem. Phys. 59, 2260 (1978).

55. J.W. Dreyer and D. Perner, Chem. Phys. Lett. 16, 169 (1972); N. van Veen, P. Brewer, P. Das, and R. Bersohn, J. Chem. Phys. 77, 4326 (1982).

56. W. Legler, Z. Physik 173, 169 (1963); K. Tachibana and A.V. Phelps, J. Chem. Phys. 71, 3544 (1979).

57. D.J. Burns, D.E. Golden, and D.W. Galliart, J. Chem. Phys. 65, 2616 (1976); A.B. Wedding, H.A. Blevin, and J. Fletcher, J. Phys. D 18, 2361 (1985).

58. S.V. Filseth, R. Wallenstein, and H. Zacharais, Opt. Commun. 23, 231 (1977); K.L. Carleton, K.H. Welge, and S.R. Leone, Chem. Phys. Lett. 115, 492 (1985).

59. R.A. Gottscho, A. Mitchell, G.R. Scheller, N.L. Schryer, D.B. Graves, and J.P. Boeuf, Electrochem. Soc. 88-22, 1 (1988).

60. J.P. Boeuf, J. Appl. Phys. 63, 1342 (1988); T.J. Sommerer, W.N.G. Hitchon, and J.E. Lawler, Phys. Rev. A 39, 6356 (1989).

61. V.T. Gylys, B.M. Jelenković, and A.V. Phelps, J. Appl. Phys. 65, 3369 (1989).

 ☆U.S. GOVERNMENT PRINTING OFFICE: 1990 - 748-056/24539